Electronic Supplementary Material (ESI) for Dalton Transactions.

Electronic Supplementary Information

A manganese (II) phthalocyanine under water-oxidation reaction: New findings

Younes Mousazade[a], Mohammad Mahdi Najafpour[a-c*], Robabeh Bagheri[d], Zvonko Jagličić[e], Jitendra Pal Singh[f], Keun Hwa Chae[f], Zhenlun Song[d], Margarita V. Rodionova[g], Roman A. Voloshin[g], Jian-Ren Shen[h,i], Seeram Ramakrishna[j*] and Suleyman I. Allakhverdiev[g,k-n*]

[a]*Department of Chemistry, Institute for Advanced Studies in Basic Sciences (IASBS), Zanjan, 45137-66731, Iran*

[b]*Center of Climate Change and Global Warming, Institute for Advanced Studies in Basic Sciences (IASBS), Zanjan, 45137-66731, Iran*

[c]*Research Center for Basic Sciences & Modern Technologies (RBST), Institute for Advanced Studies in Basic Sciences (IASBS), Zanjan 45137-66731, Iran*

[d]*Surface Protection Research Group, Surface Department, Ningbo Institute of Materials Technology and Engineering, Chinese Academy of Sciences, 519 Zhuangshi Road, Ningbo 315201, China*

[e]*Institute of Mathematics, Physics and Mechanics & Faculty of Civil and Geodetic Engineering, University of Ljubljana, Jadranska 19, SI-1000 Ljubljana, Slovenia*

[f]*Advanced Analysis Center, Korea Institute of Science and Technology (KIST), Seoul 02792, Republic of Korea*

[g]*Controlled Photobiosynthesis Laboratory, Institute of Plant Physiology, Russian Academy of Sciences, Botanicheskaya Street 35, Moscow 127276, Russia.*

[h]*Research Institute for Interdisciplinary Science and Graduate School of Natural Science and Technology, Okayama University, Okayama 700-8530, Japan.*

[i]*Photosynthesis Research Center, Key Laboratory of Photobiology, Institute of Botany, Chinese Academy of Sciences, No. 20, Nanxincun, Xiangshan, Beijing 100093, China.*

[j]*Department of Mechanical Engineering, Center for Nanofibers and Nanotechnology, National University of Singapore, Singapore, 117576, Singapore.*

[k]*Bionanotechnology Laboratory, Institute of Molecular Biology and Biotechnology, Azerbaijan National Academy of Sciences, Matbuat Avenue 2a, Baku 1073, Azerbaijan*

[l]*Institute of Basic Biological Problems, Russian Academy of Sciences, Pushchino, Moscow Region, 142290, Russia.*

[m]*Department of Plant Physiology, Faculty of Biology, M.V. Lomonosov Moscow State University, Leninskie Gory 1-12, Moscow 119991, Russia.*

[n]*Moscow Institute of Physics and Technology, Institutsky lane 9, Dolgoprudny, Moscow Region 141700, Russia.*

*Corresponding authors: E-mail: *mmnajafpour@iasbs.ac.ir; suleyman.allakhverdiiev@gmail.com*

Table of Contents

Experimental Section

Materials
All reagents and solvents were obtained from commercial sources and used without further purification. Fluorine doped tin oxide coated glass (FTO) and manganese (II) phthalocyanine were purchased from Sigma-Aldrich Company. Glassy carbon electrodes were purchased from Azar Electrode Company. 3,4,5-trihydroxy benzoic, $Mn(CH_3COO)_2.4H_2O$ was purchased from Merck Company. Tetraethylammonium Perchlorate was purchased from ACROS Organics. High purity deionized water was obtained by passing distilled water through a nanopore Milli-Q water purification system.

Instrumentation
Scanning electron microscopy (SEM) and atomic force microscopy (AFM) were carried out with LEO 1430VP and Dualscope/ Rasterscope C26, DME, respectively. The X-ray powder diffraction patterns were recorded with a Bruker, D8 ADVANCE (Germany) diffractometer (CuK_α radiation). Energy dispersive X-ray spectrometry (EDX) analysis/mapping was carried out with a scanning electron microscope CamScan 4DV (CamScan UK). Electrochemical experiments were performed using an EmStat3+ from PalmSens (Netherlands). The distance between two opposite sides of the foil electrode was measured by a digital caliper MarCal 16ER model (Mahr, Germany). The temperature was measured by Laser liner 082 (Germany). FTIR spectra of KBr pellets of compounds were recorded on a
Bruker vector 22 in the range between 400 and 4000 cm^{-1}. Operando visible Spectro-electrochemistry was recorded by a mini spectrophotometer (Pooyesh Tadbir Karaneh (Phystec), Iran). Gas Chromatography/Mass Spectrometery was carried out with Gas Chromatography/Mass Spectrometer GC: 6890 (MSD: 5973) (Agilent, USA). Details of sample preparation for GC-Mass spectroscopy has been presented at experimental section as 'Decomposition products extraction'.

Cyclic voltammetry
For investigation of the electrochemical behavior of **1**, cyclic voltammetry in a three-electrode cell was performed in which Ag/AgCl, platinum sheet and FTO was used as a reference, counter and working electrode respectively. A solution of tetraethylammonium perchlorate (0.25 M; Caution: perchlorate salts of organic compounds are potentially explosive. Only a small amount of material should be prepared and handled with caution) in water: acetonitrile with 1:3 ratio was prepared as electrolyte and 10 mg of **1** was added to 25 ml of this solution and this mixture was stirred for 10 min. The mixture was centrifuged to remove undissolved solids. Cyclic voltammetry was performed in the range of 0 to 1.7 V at room-temperature and 50.0 mVs^{-1} scan rate.

Amperometry
A solution of tetraethylammonium perchlorate (0.25 M) in water: acetonitrile with 1:3 ratio according to the last section was prepared and 10 mg of **1** was added, mixed and after 10 min centrifuged. Amperometry measurement was performed in two separated cells which connected by a salt bridge. The complex solution was set as anodic half-cell and an aqua solution of $LiClO_4$ (0.25 M) was used as cathodic half-cell. 1.6 V potential was applied for 1.5 h. To prepare the sample for different analysis, the amperometry determination was applied for 10 h. The formed MnO_x was scratched from the FTO surface and collected for different analysis.

Investigation of FTO-1
After 1.5h amperometry determination, a very thin layer MnO_x was formed on FTO electrode surface. This FTO/MnO_x was investigated in a fresh electrolyte. Cyclic voltammetry was performed for 15 cycles. In the same way, a new FTO/MnO_x system was prepared and amperometry determination was performed at 1.6 V vs. Ag/AgCl reference electrode in a fresh electrolyte by a three-electrode cell. To compare catalytic activity between complex **1**, MnO_x and FTO, cyclic voltammetry and amperometry of a new solution of electrolyte using a fresh FTO at the absent of **1** were performed and obtained data were figured out.

Amperometry and in-situ visible spectroscopy
In situ visible spectroscopy was measured using a $1cm^2$ spectrophotometric cell and setting three-electrode in the cell. To the electrolyte solution of complex, 1.6 V potential was applied and every 10 min visible absorption of the solution was recorded.

Decomposition products extraction
To the determination of decomposition products, amperometry was continued until the solution became colorless. Then 10 ml CH_2Cl_2 was added to the solution for extraction of the organic components. Extraction was repeated two times more. The organic layer was separated and evaporated at room temperature. Solid phase dissolved in

20 ml dichloromethane, filtered and evaporated at room temperature again. Obtained solids were collected for GC-mass analysis.

Magnetization measurements
Magnetization was measured between 2 K and 300 K in a constant magnetic field of 10 mT, and as a function of magnetic field at 300 K and 2 K using a Quantum Design MPMS-XI-5 SQUID magnetometer.

The mass ratio of the manganese per mass of the FTO
To estimate the mass ratio of the manganese per mass of the FTO, the M(H) curve for FTO-**1** was fitted with a sum of a linear function that accounts for the diamagnetic part, and Langevin function that phenomenological describes the ferromagnetic, "S" part of the M(H):

$$M(H) = k \cdot H + M_s L\left(\frac{\mu H}{k_B T}\right)$$

If we take 4 μB per Mn ion as measured in **1** and this value is close to the spin only magnetic moment of Mn(III) (5.0 μB,) and Mn(IV) (3.9 μB), the saturation magnetization per kilogram of manganese is approximately 400 Am^2/ kg. Comparing with the measured Ms = 1.3·10-3 Am^2/kg we obtain that approximately (1.3·10-3 Am^2/kg)/(400 Am^2/kg) = 3·10-4 % of the mass of FTO-**1** is manganese.

Oxygen-evolution measurements
The measurements were carried out at 25.0 ºC using an optical-probe oxygen meter (HQ40d from Hach, Düsseldorf, Germany).

Experimental Details for X-ray absorptions
The extended edge X-ray absorption fine structure (EXAFS) measurements on FTO-**1** and reference materials (Mn oxides) were performed at the hard X-ray 1D XAS KIST-PAL beamline, Pohang accelerator laboratory, operating at 3.0 GeV with a maximum storage current of 320 mA. 1D XAS KIST-PAL beamline is a bending magnet X-ray Scattering (XRS) beamline which uses Si(111) double crystal monochromator to give a wide range of monochromatic energies (4-16 keV). To measure EXAFS spectra of these materials, higher harmonics were removed by detuning incident beam intensity to 60% of maximum intensity. The ionization chamber filled with He was used to record the intensity of the incident X-rays. The fluorescence EXAFS signal was measured by a passivated implanted planar silicon (PIPS) detector. Before the measurement, reference samples (Mn oxides) is used for energy calibration. Under stationary conditions, extended X-ray absorption fine-structure (EXAFS) measurements were performed at the Mn *K*- edge in the step scanning mode. The program Athena was used to identifying the beginning of the absorption edge (E_0), fit pre- and post-edge backgrounds, and hence to obtain the normalized absorbance χ as a function of the modulus of the photoelectron wave vector k. The fitting was carried out using ARTEMIS in the k range 3-10.5 Å. The EXAFS data is Fourier transformed to R-space to investigate the atomic structure and relative bond-lengths with respective to absorbing atoms. The theoretical structure for reference oxides was generated using the ATOM. In the fitting, values of coordination number (N), bond length (R_i) and Debye-Waller (σ_2) factors are kept free. The parameter ε_o, which is a correction to edge energy, was free to vary in all fitting. The errors in the fit parameters of R_i and σ_2 were obtained from 90% of goodness factor as calculated in IFEFFIT.

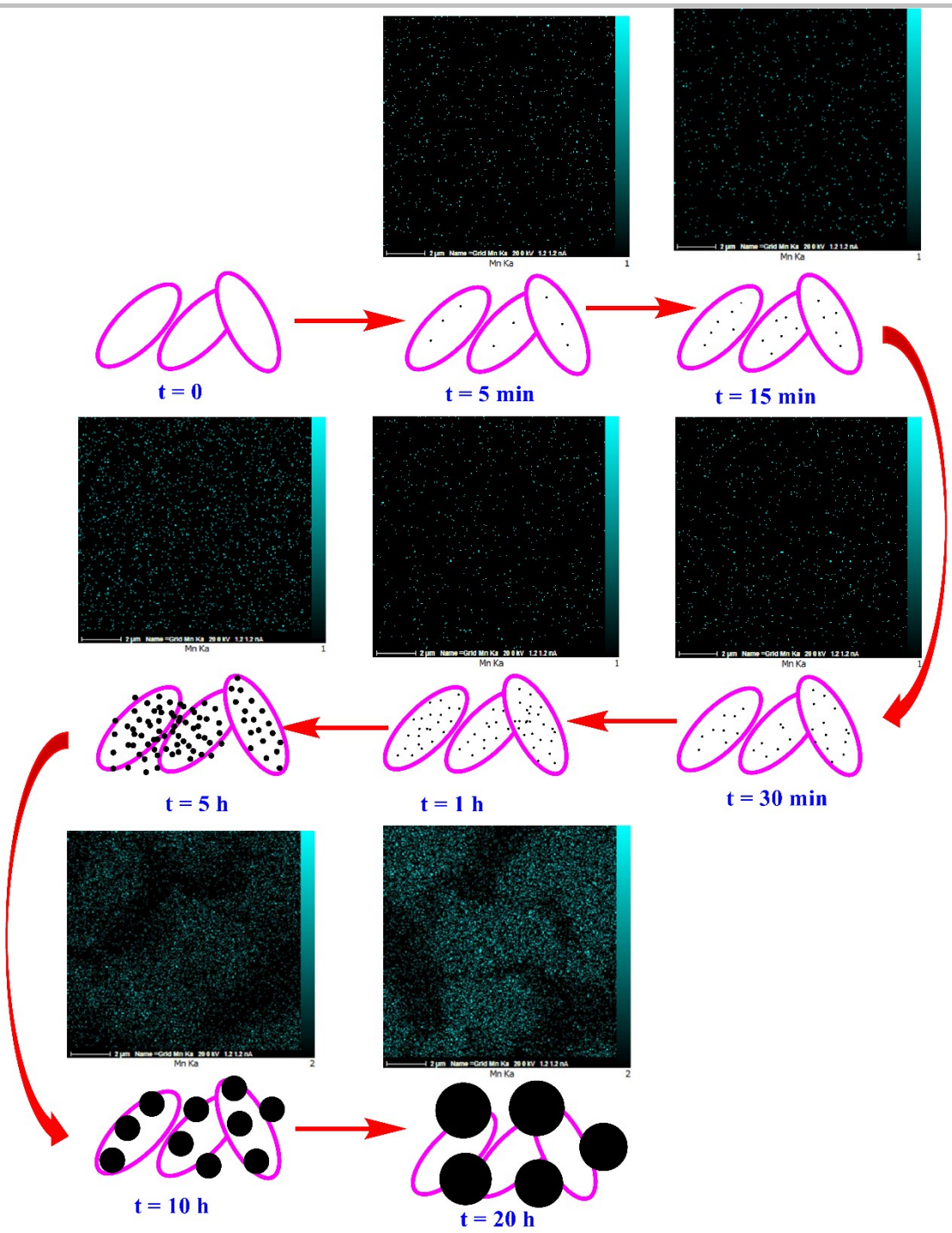

Scheme S1 Proposed mechanism to form Mn oxide on the surface of FTO and attributed EDX-SEM images (Mn: cyan).

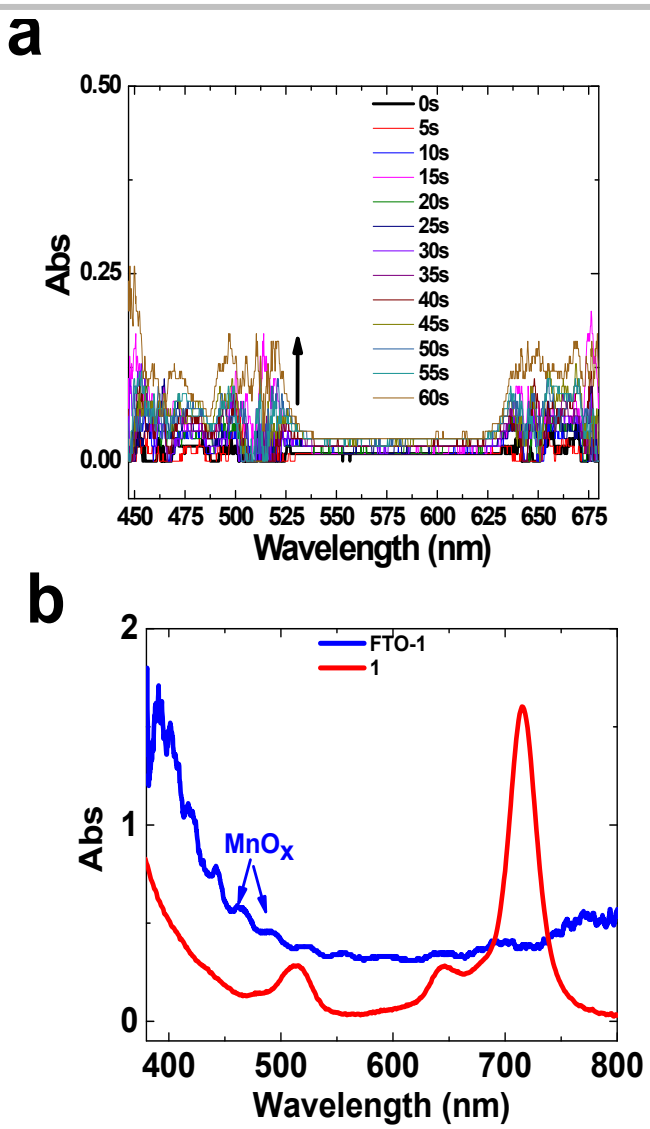

Figure S1 Time-variation in situ visible spectra of FTO surface during amperometry of **1** at 1.6V for one minute. In all cases, reference and counter electrodes were Ag/AgCl and Pt sheet respectively (a). UV-Vis spectra for FTO-**1** and **1** (b).

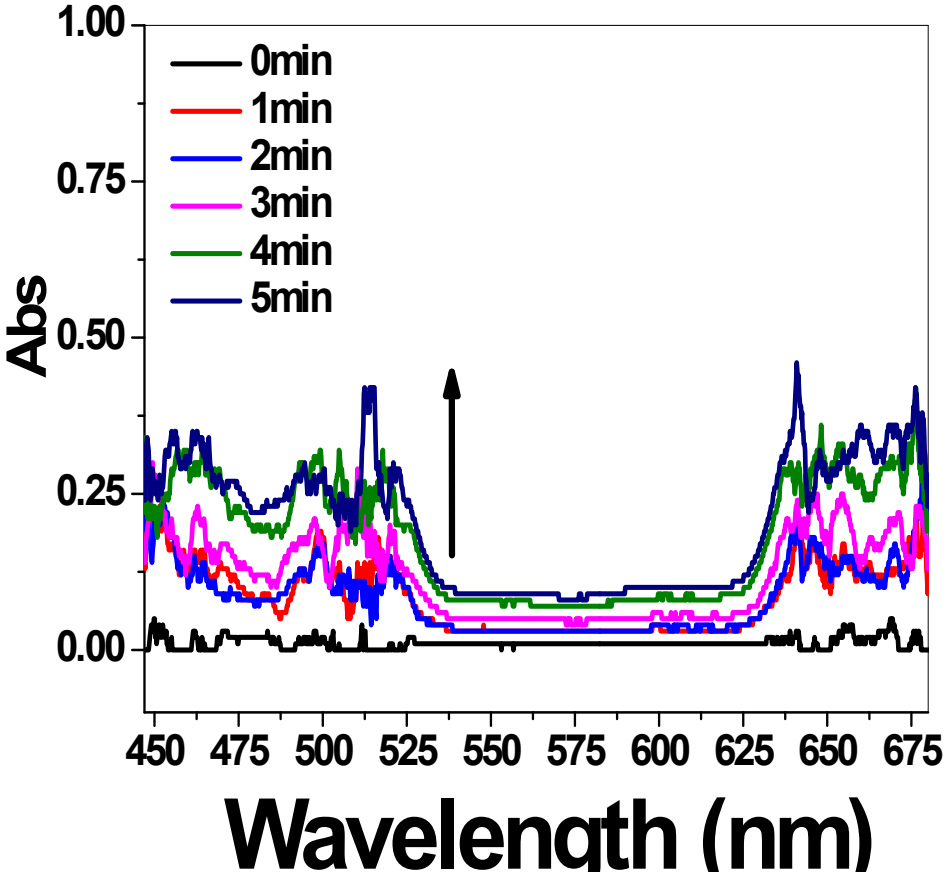

Figure S2 Time-variation in situ visible spectra of FTO surface during amperometry of **1** at 1.6V for 5 minutes. In all cases, reference and counter electrodes were Ag/AgCl and Pt sheet respectively.

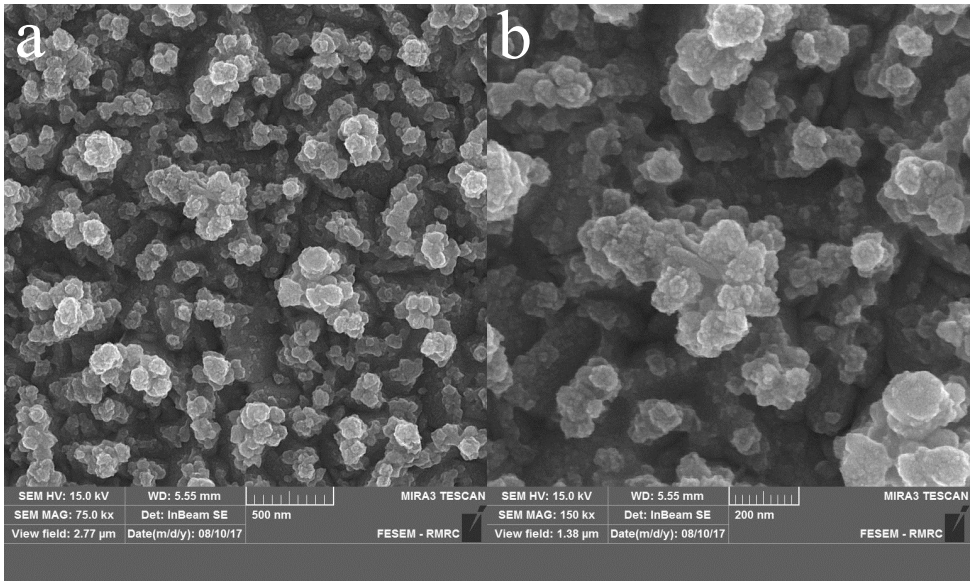

Figure S3 SEM image from FTO-**1** in the absence of EDTA (a, scale bar: 500 nm; b, scale bar:200 nm).

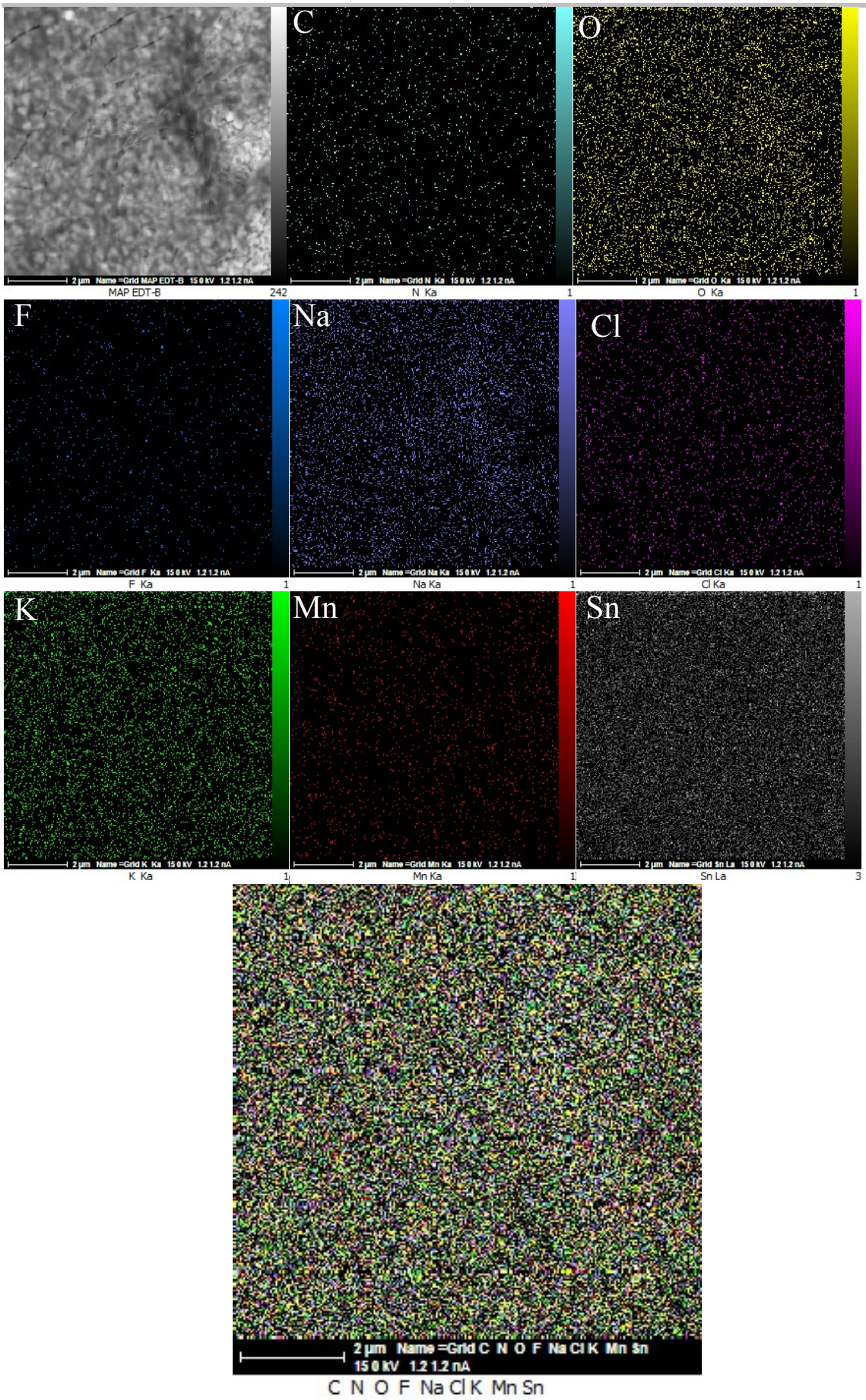

Figure S4 EDX-SEM image from FTO-**1** in the absence of EDTA. Scale bar for all images is 2 µm.

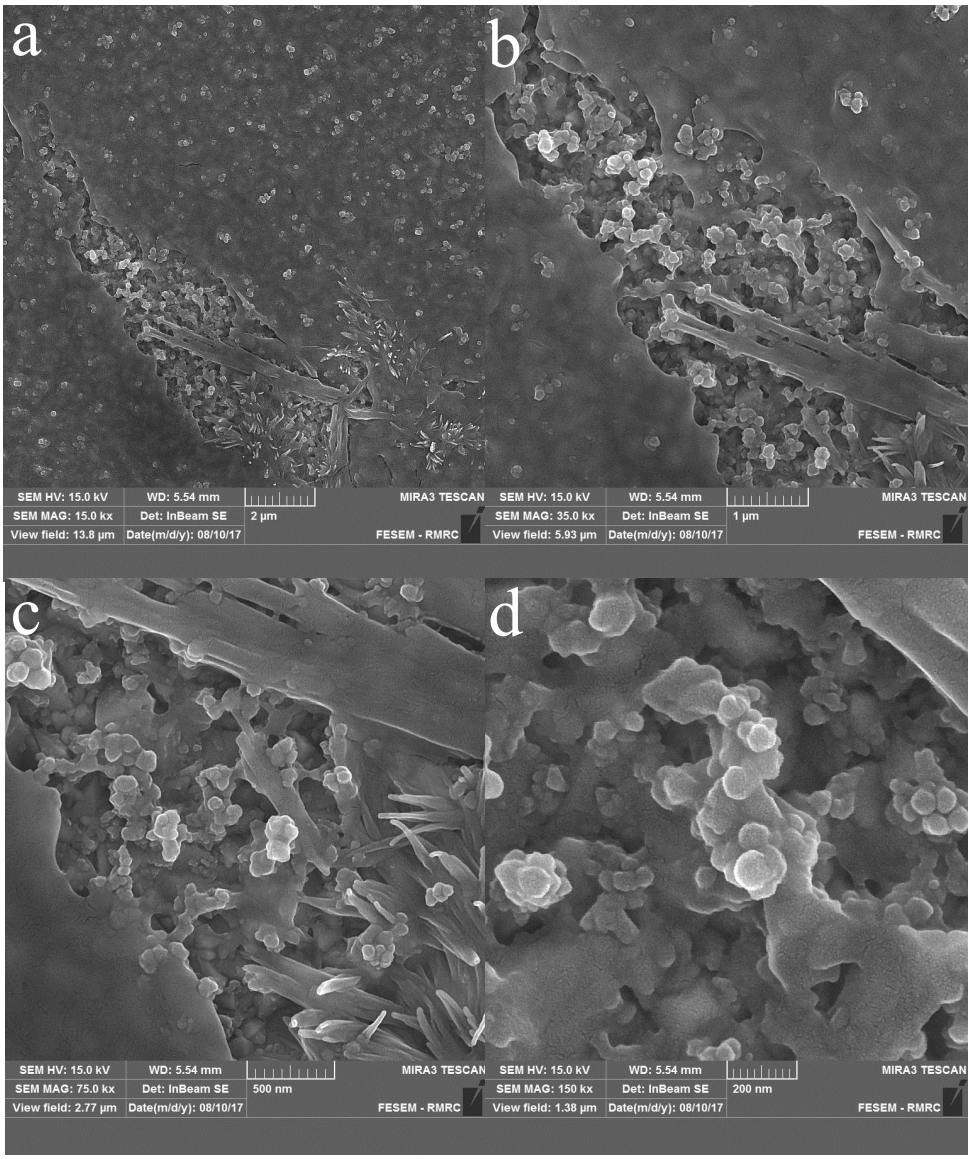

Figure S5 SEM image from FTO-**1** in the presence of EDTA (a, scale bar: 2 µm; b, scale bar: 1 µm c, scale bar:500 nm; d, scale bar:200 nm).

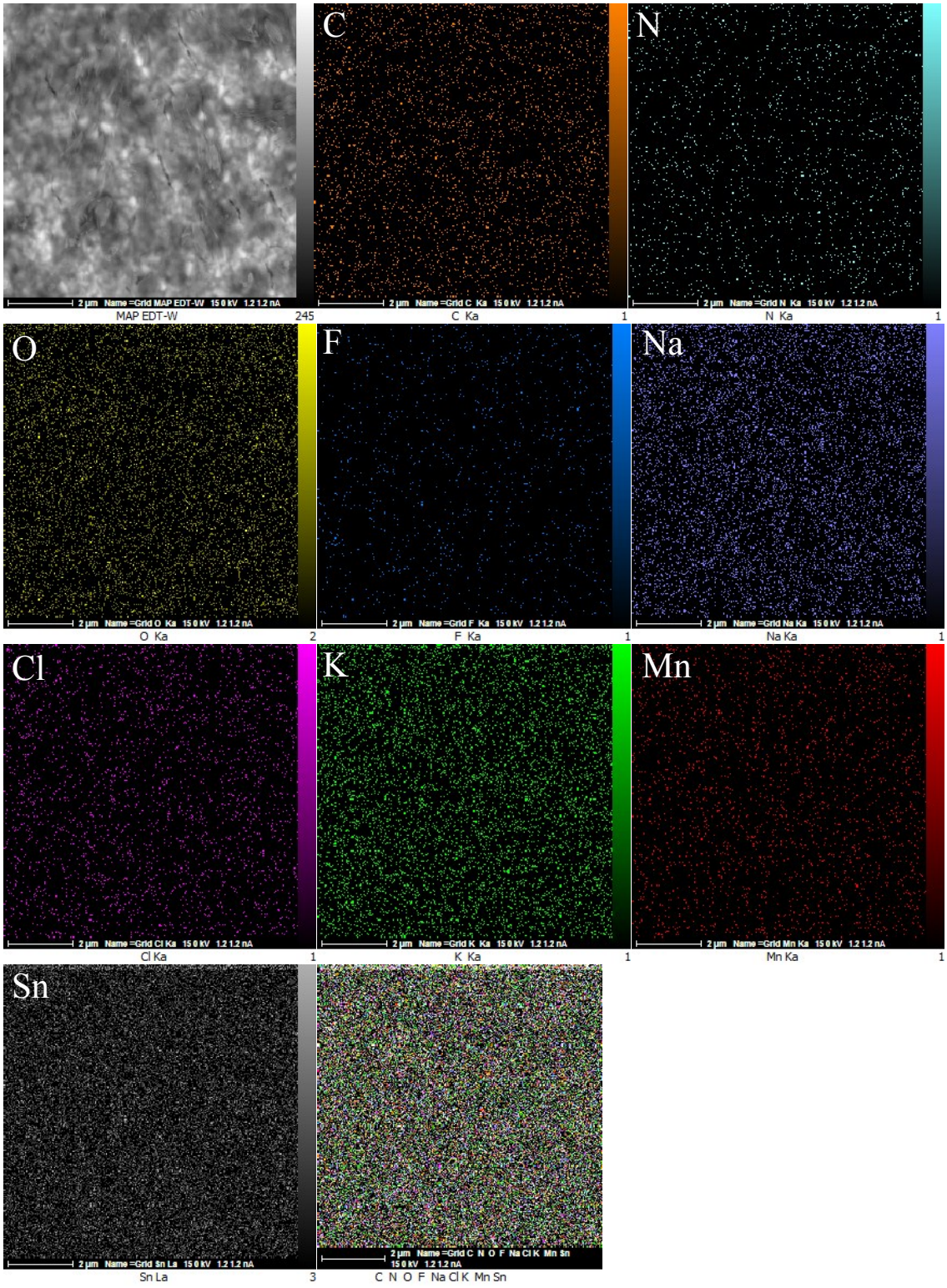

Figure S6 EDX-SEM image from FTO-**1** in the presence of EDTA. Scale bar for all images is 2 μm.

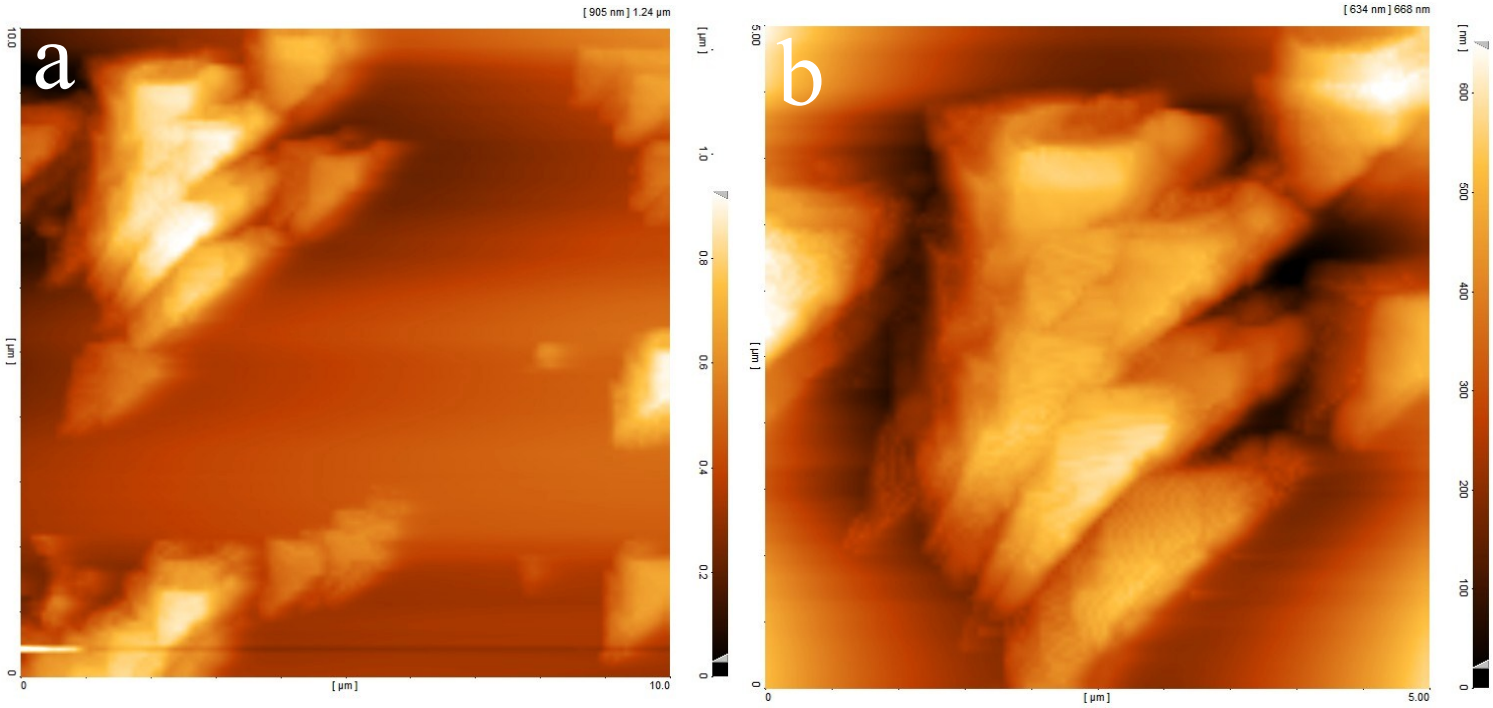

Figure S7 AFM images from fresh FTO with different scale bars (a,b).

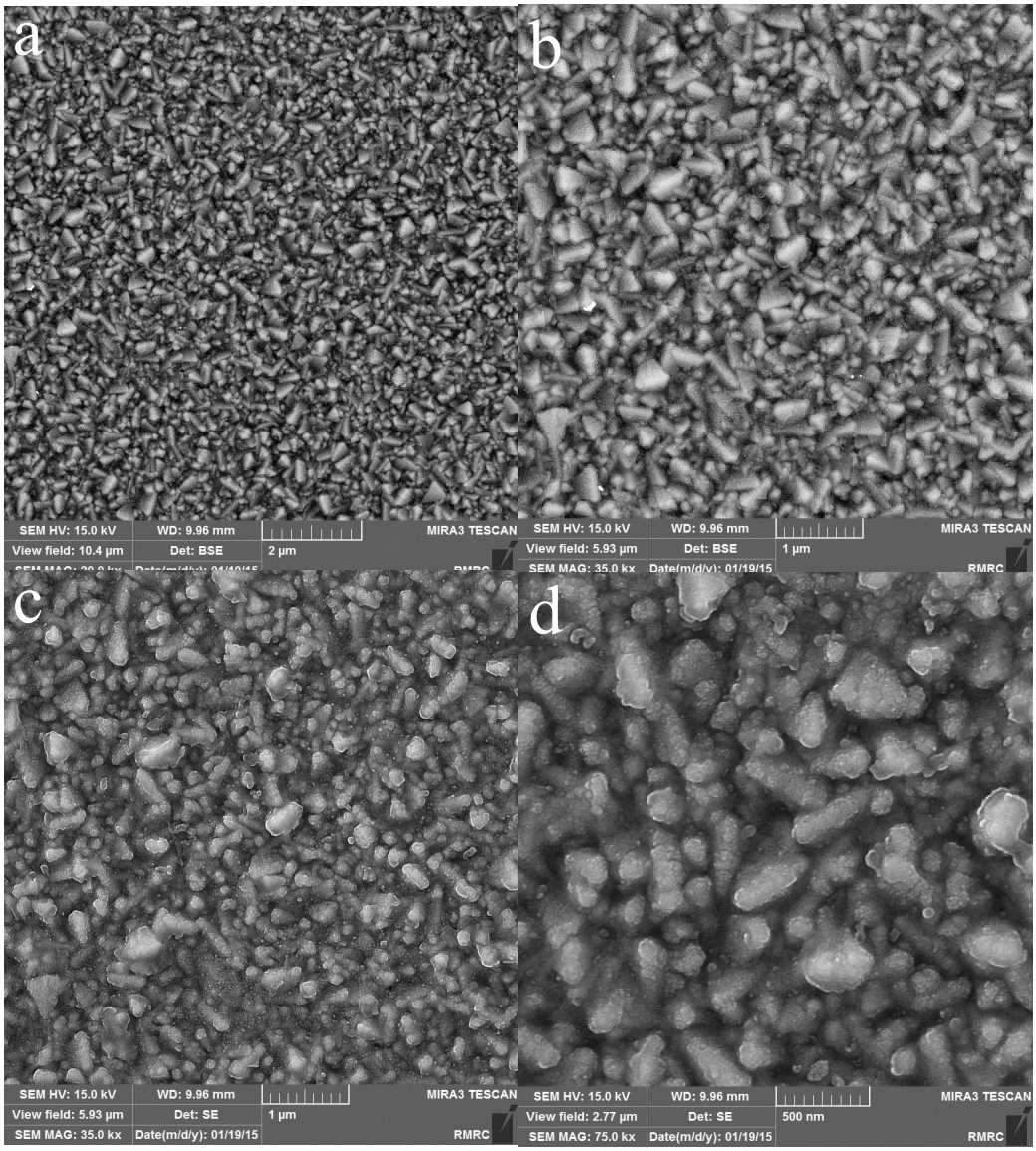

Figure S8 SEM images from fresh FTO (a, scale bar: 2 μm; b, scale bar: 1 μm; c, scale bar: 1 μm; d, scale bar: 500 nm).

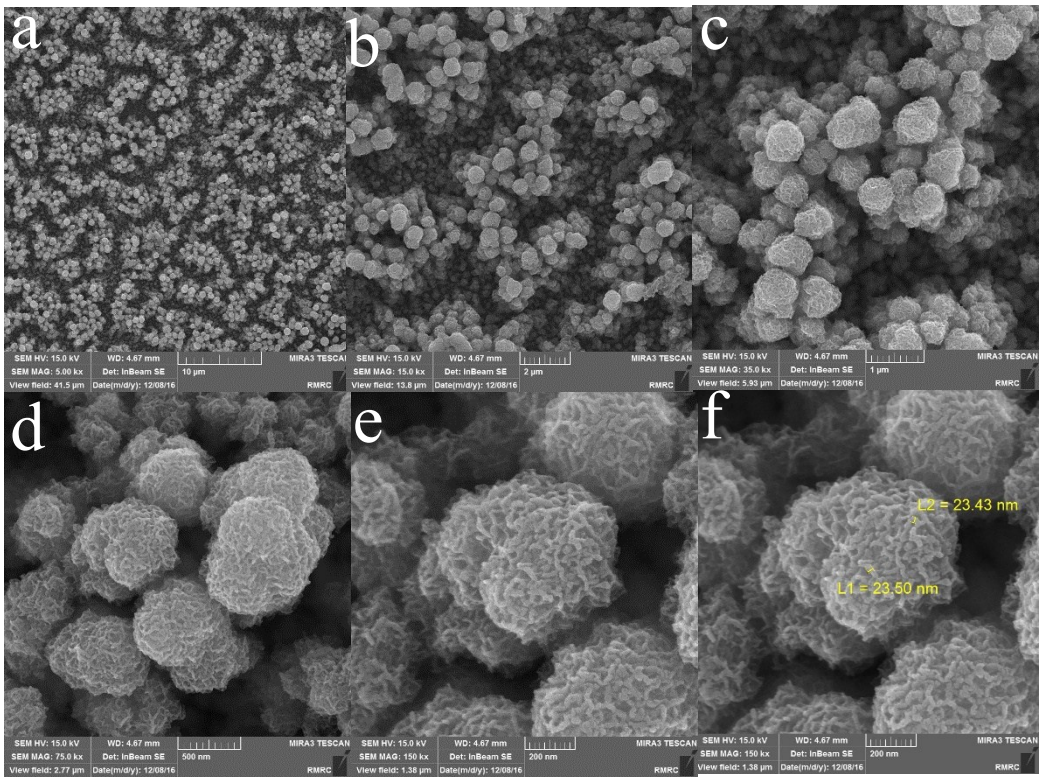

Figure S9 SEM images from the surface of as prepared FTO-**1** after 10h amperometry of a solution of **1 (0.2 mM)** in 0.25 M Et_4NClO_4 and at 1.6V (a, scale bar: 10 μm; b, scale bar: 2 μm; c, scale bar: 1 μm; d, scale bar: 500 nm; e: scale bar: 200 nm; f: scale bar: 200 nm).

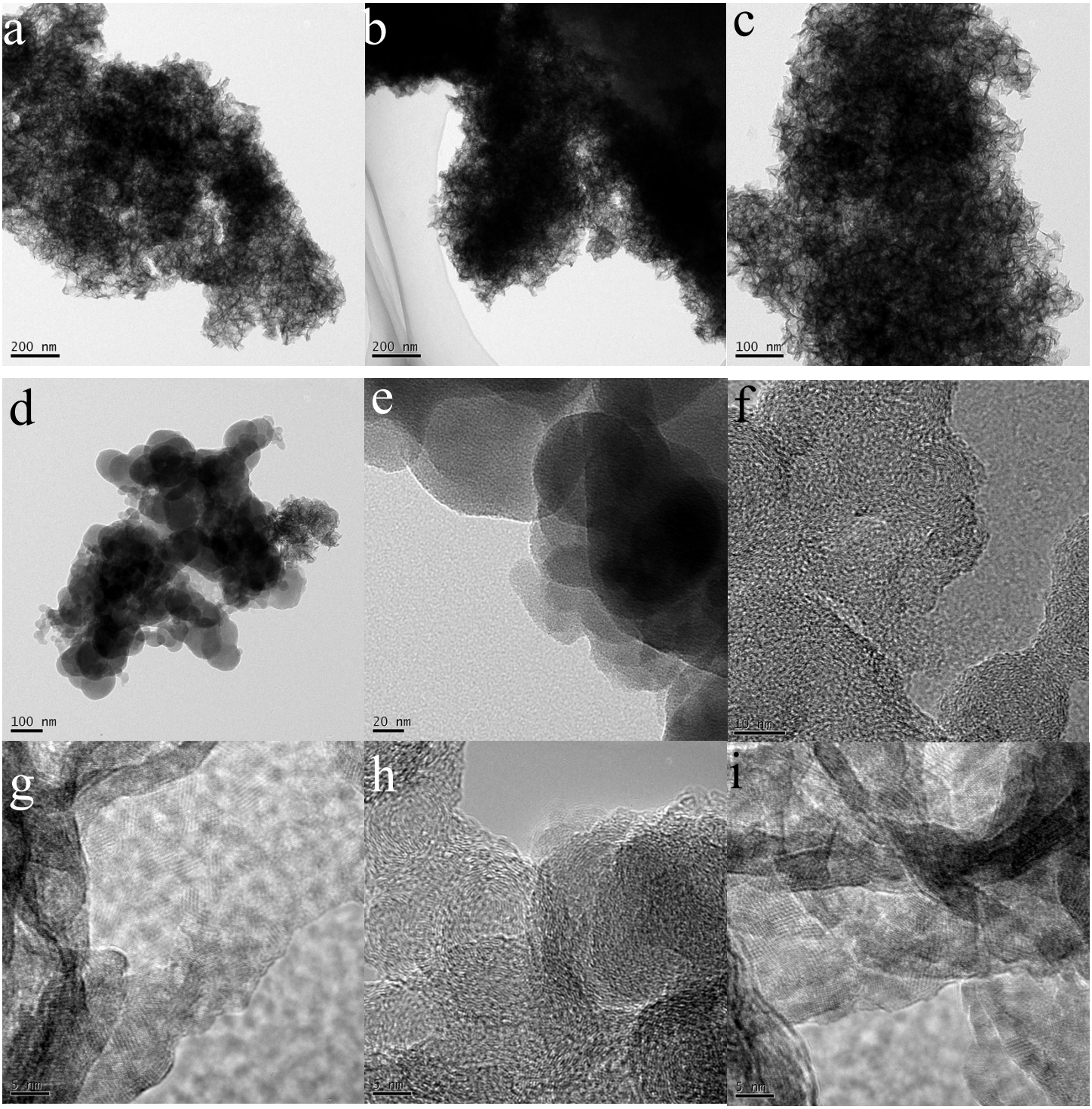

Figure S10 (HR)TEM images from mechanically separated solid from FTO-**1** after 10h amperometry of a solution of **1** (0.2 mM) in 0.25 M Et_4NClO_4 and at 1.6V (a, scale bar: 200 nm; b, scale bar: 200 nm; c, scale bar: 100 nm; d, scale bar: 100 nm; e, scale bar: 20 nm; f, scale bar: 10 nm; g: scale bar: 5 nm; h, scale bar: 5 nm; i: scale bar: 5 nm).

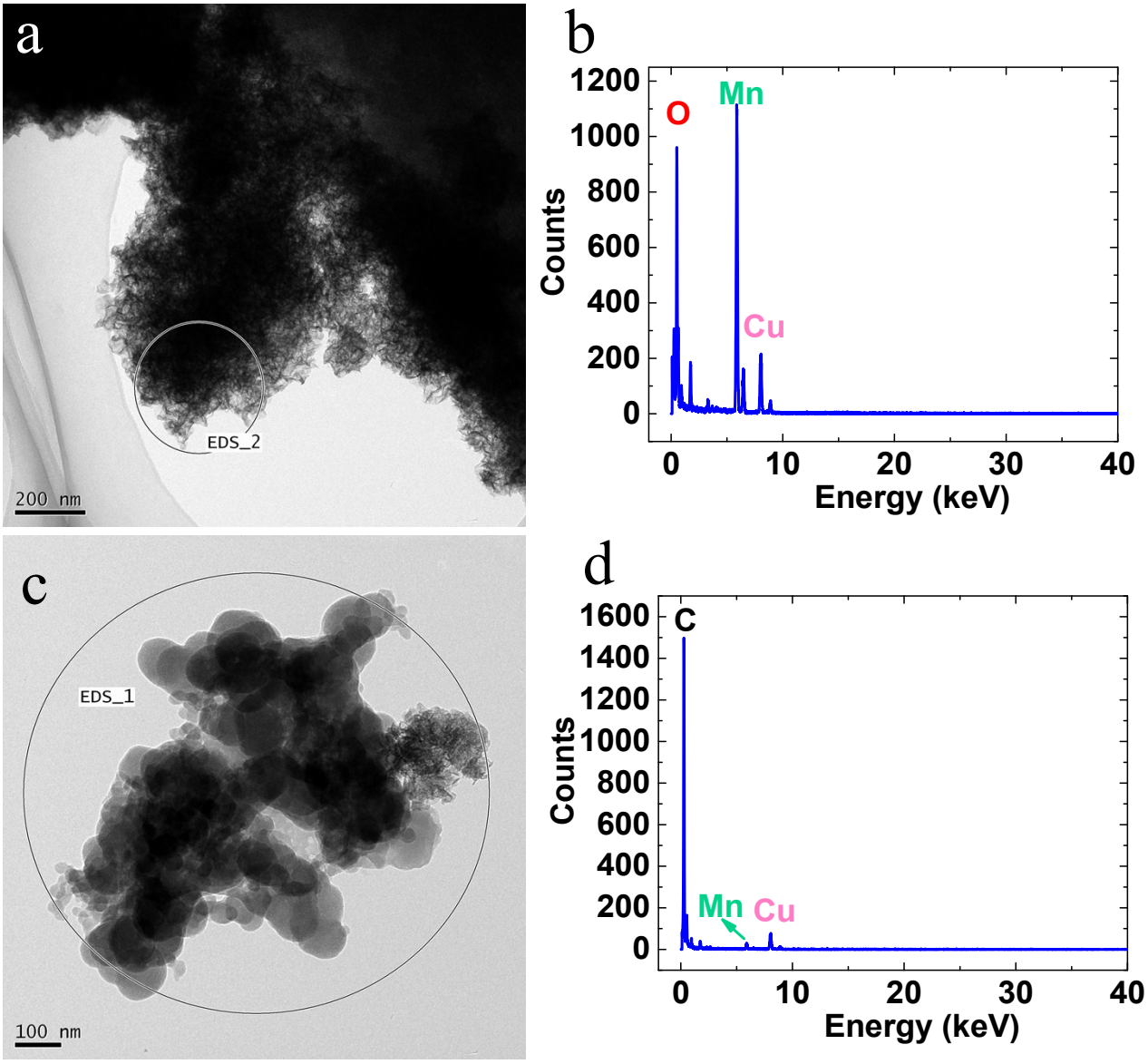

Figure S11 The EDX-TEM images. (HR)TEM images from mechanically separated solid from FTO-**1** after 10h amperometry of a solution of **1** (0.2 mM) in 0.25 M Et_4NClO_4 and at 1.6V. Inorganic area (top) and whole area (below).

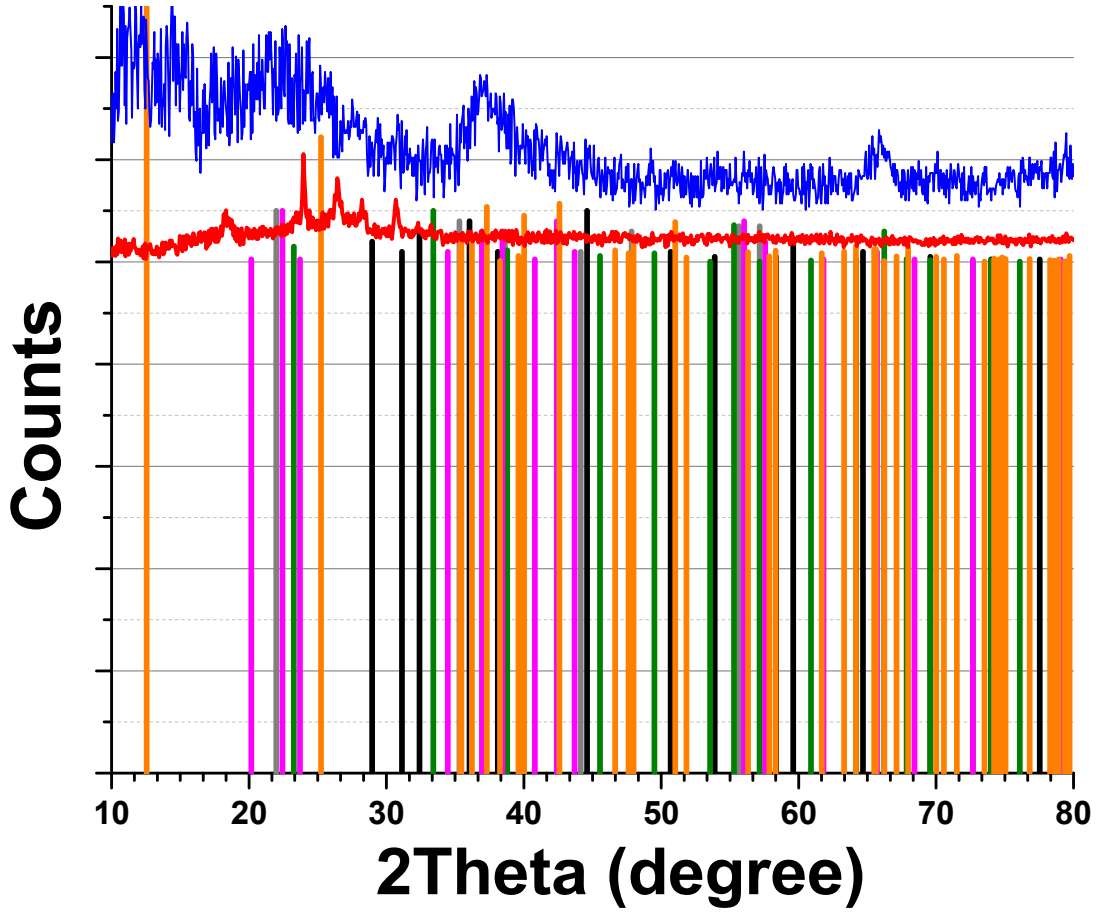

Figure S12 XRD patterns from mechanically separated solid from FTO-**1** electrode during 10 hours under water oxidation (pH = 7.0) in the bulk electrolysis of **1** at 1.5 V. MnO (000040326) (gray), Mn_3O_4 (000031041) (black), Mn_2O_3 (000011061) (olive), MnO_2 (000120713) (pink), Birnessite (010801098) (orange).

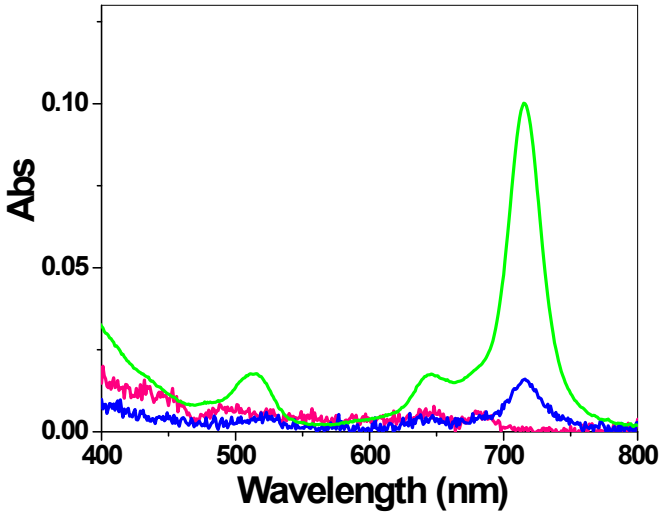

Figure S13 The treatment of FTO-**1** with phthalocyanine could form Mn phthalocyanine. FTO-**1** was placed in an acetonitrile mixture of an undissolved phetalocyanine ligand for 48 h. then liquid phase was filtrated by a GC-filter and this liquid phase was investigated via UV-Vis spectroscopy (phthalocyanine: pink; **1**: green; FTO-**1**/phthalocyanine: blue).

a

b

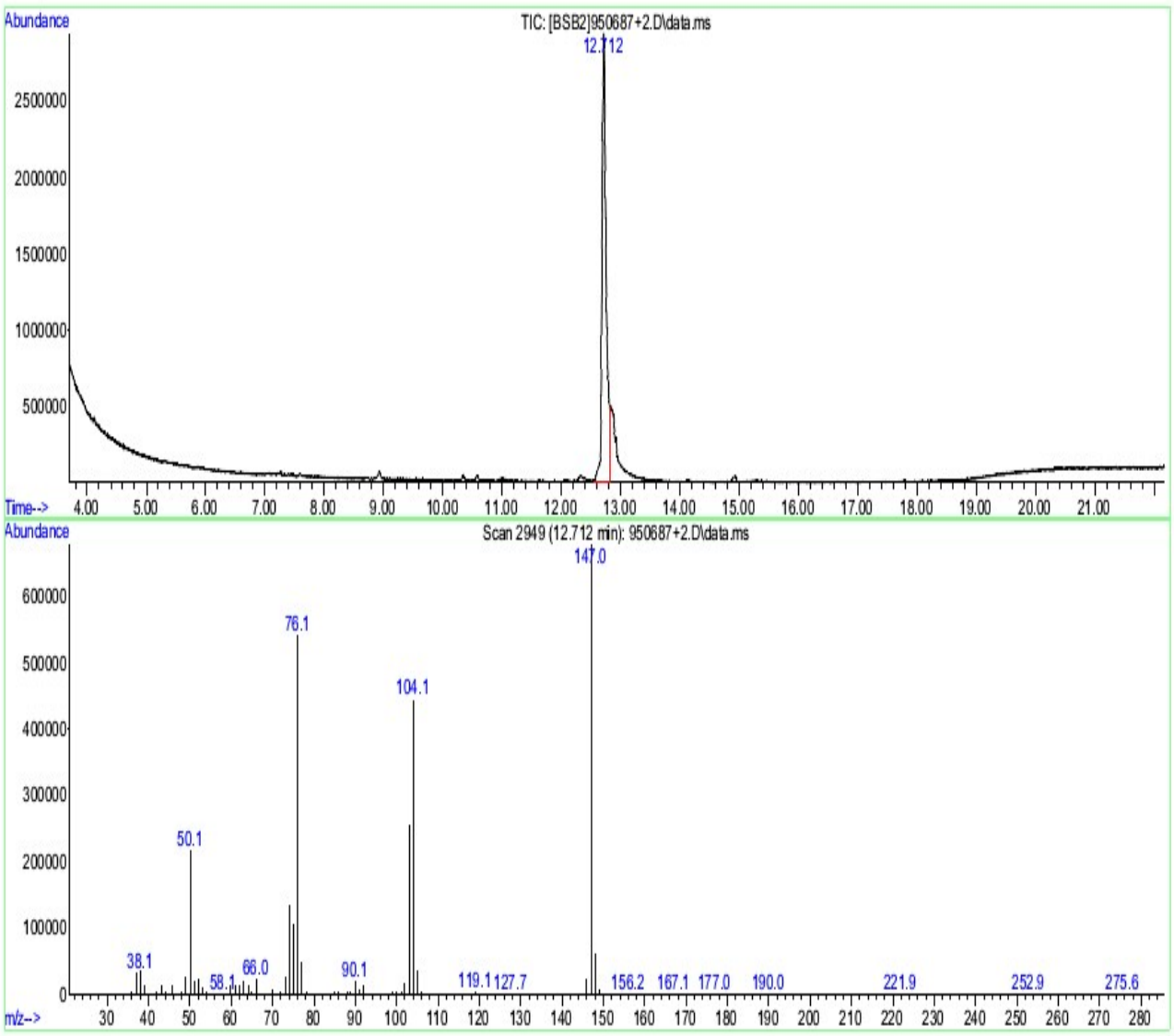

Figure S14 Gas chromatography-mass spectrometry (GC-MS) and attributed results to check for the organic compounds in solution. Gas Chromatography of extracted organic products after chronoamperometry operation (a). Mass spectroscopy pattern for organic products manifesting at time of fly 12.72 min in GC. Suggested structures and mass spectroscopy patterns of products according to the sample patterns (2-cyanobenzoeic acid (c); phthalimide (d)).

c

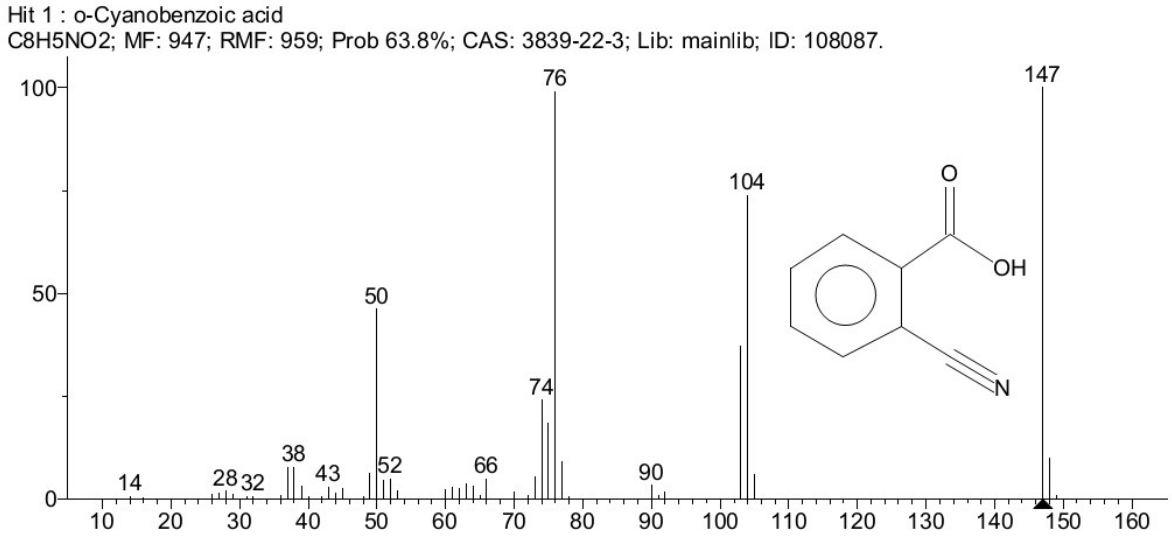

d

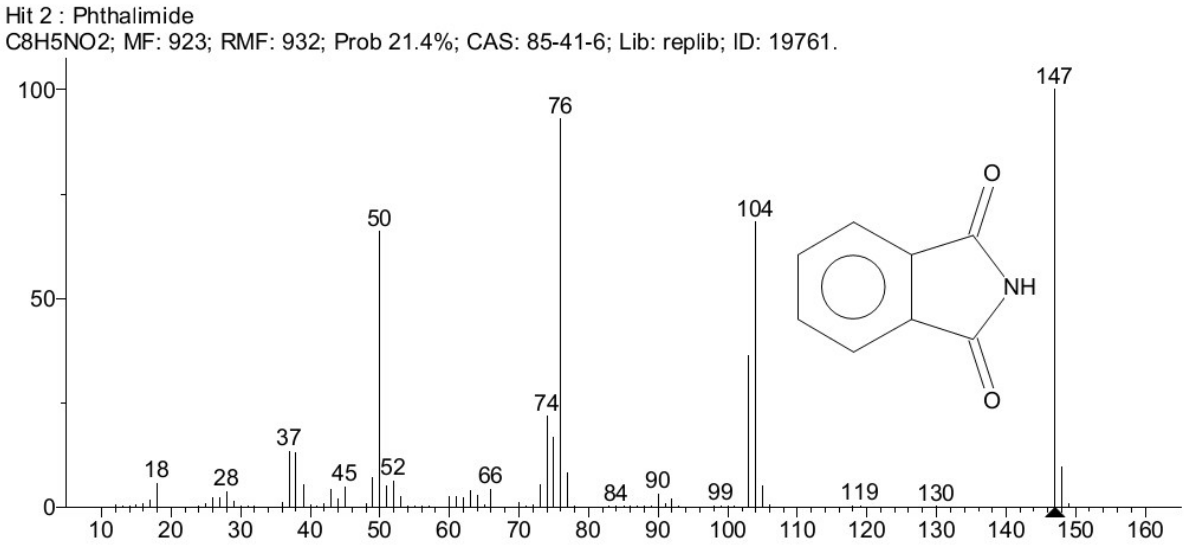

Figure S14 (continue).

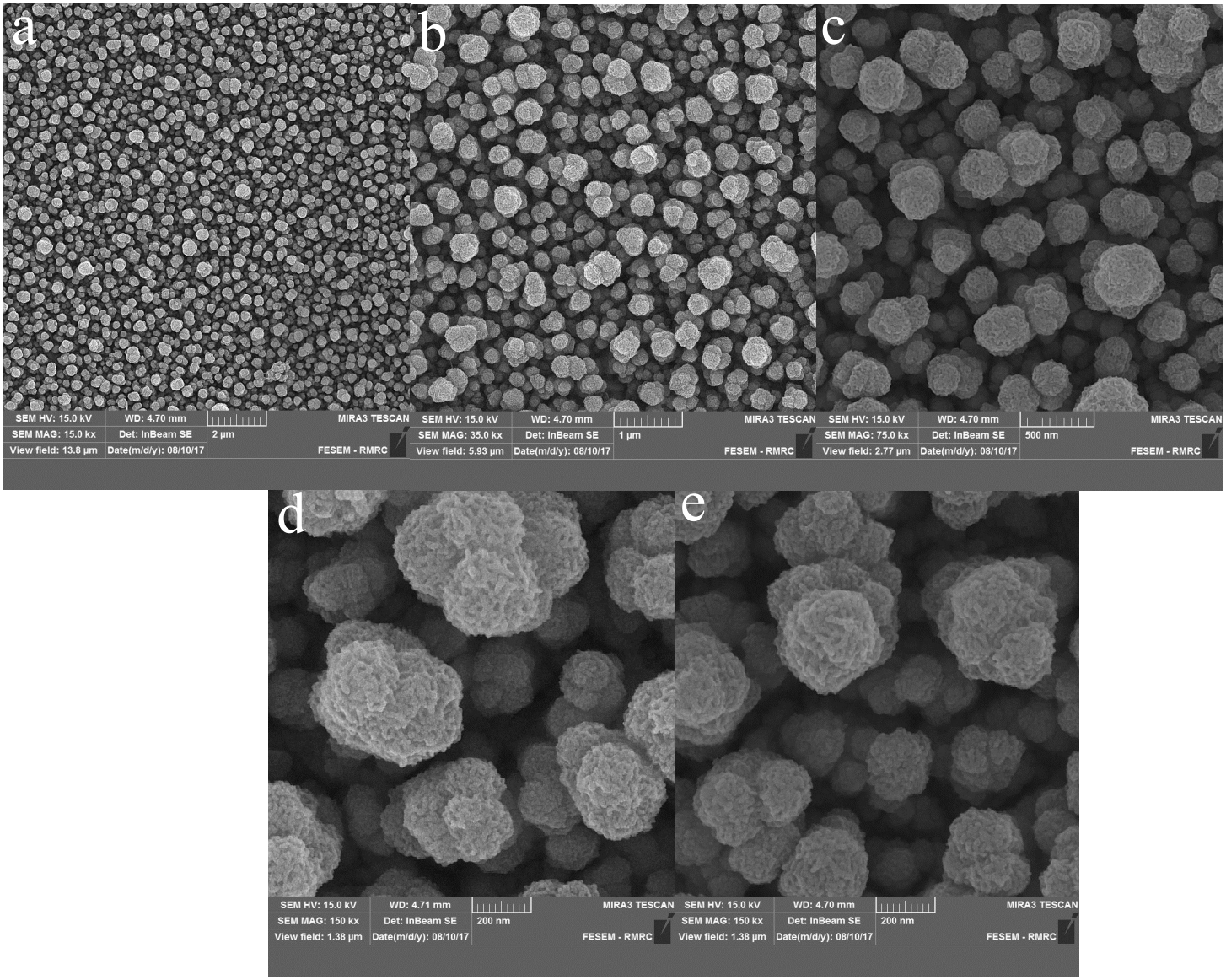

Figure S15 SEM image from FTO in the presence of 2-cyanobenzoeic acid:Mn(II) with the ratio 4:1 respectively and after 2h amperometry in 0.25 M Et_4NClO_4 solution and at 1.6V (a, scale bar: 2 µm; b, scale bar: 1 µm; c, scale bar: 500 nm; d: scale bar: 200 nm; e: scale bar: 200 nm).

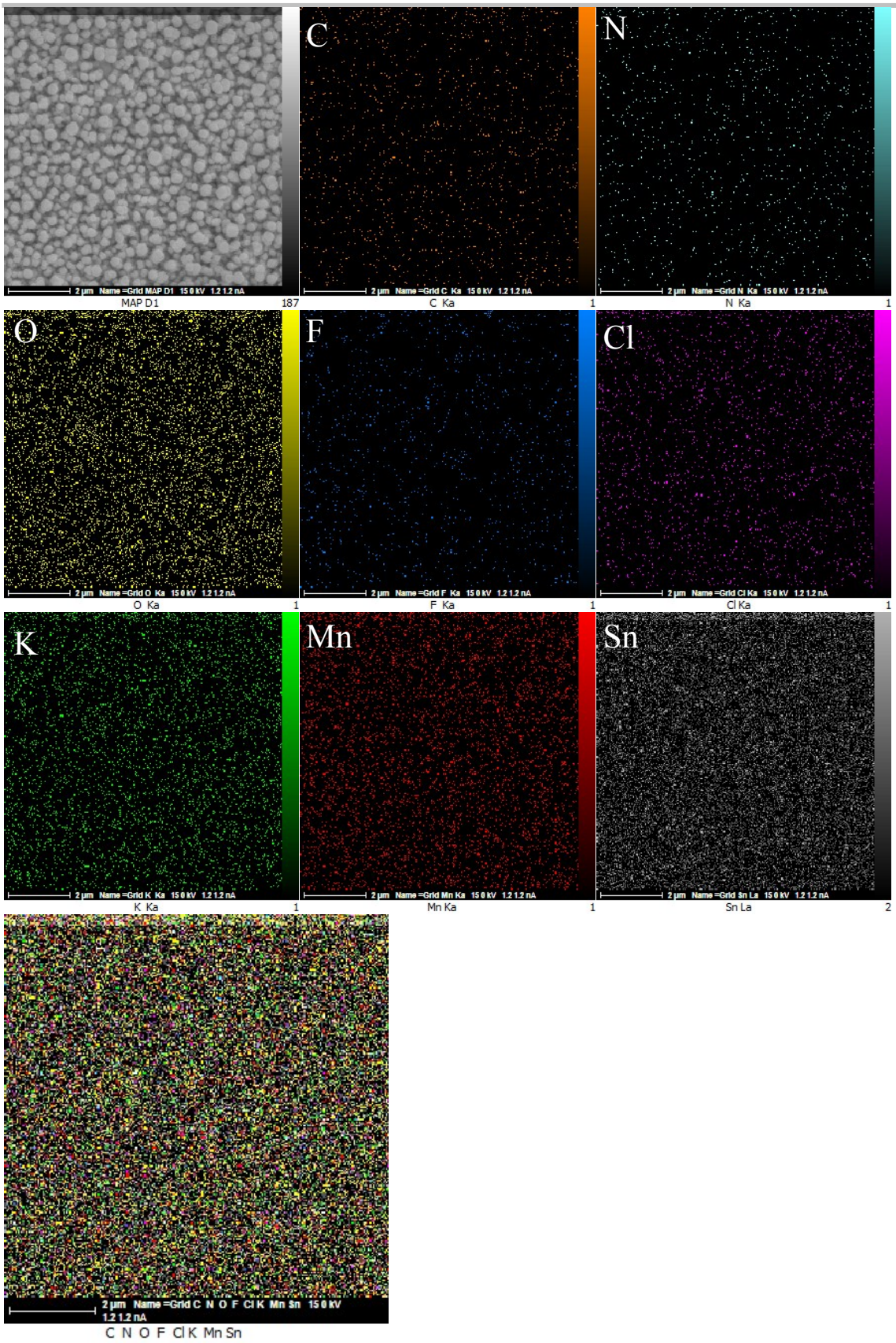

Figure S16 EDX-SEM image from FTO in the presence of 2-cyanobenzoeic acid:Mn(II) with the ratio 4:1 respectively and after 2h amperometry in 0.25 M Et_4NClO_4 solution and at 1.6V. Scale bar for all images is 2 μm.

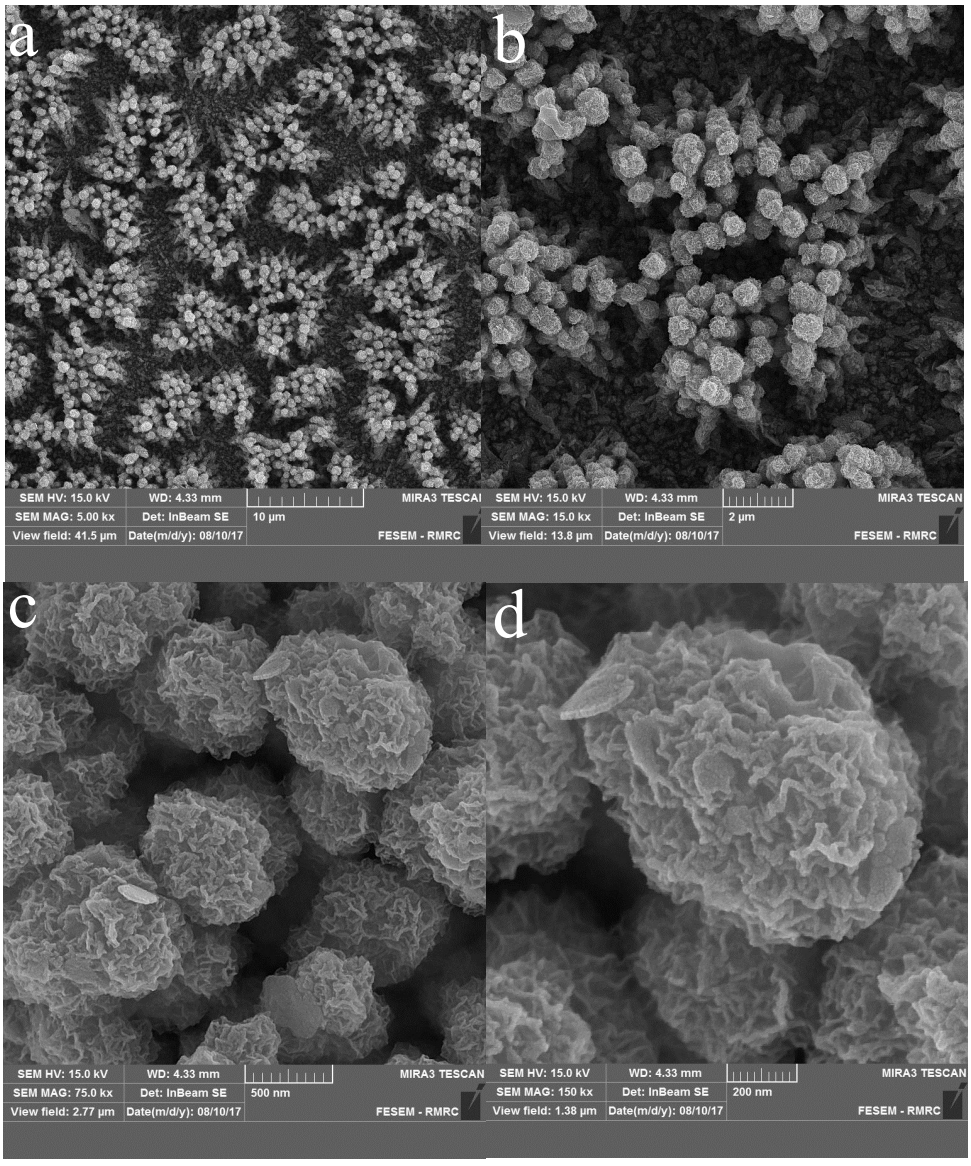

Figure S17 SEM image from FTO in the presence of phthalimide:Mn(II) with the ratio 4:1 respectively and after 2h amperometry in 0.25 M Et_4NClO_4 solution and at 1.6V (a, scale bar: 10 µm; b, scale bar: 2 µm; c, scale bar: 500 nm; d, scale bar: 200 nm).

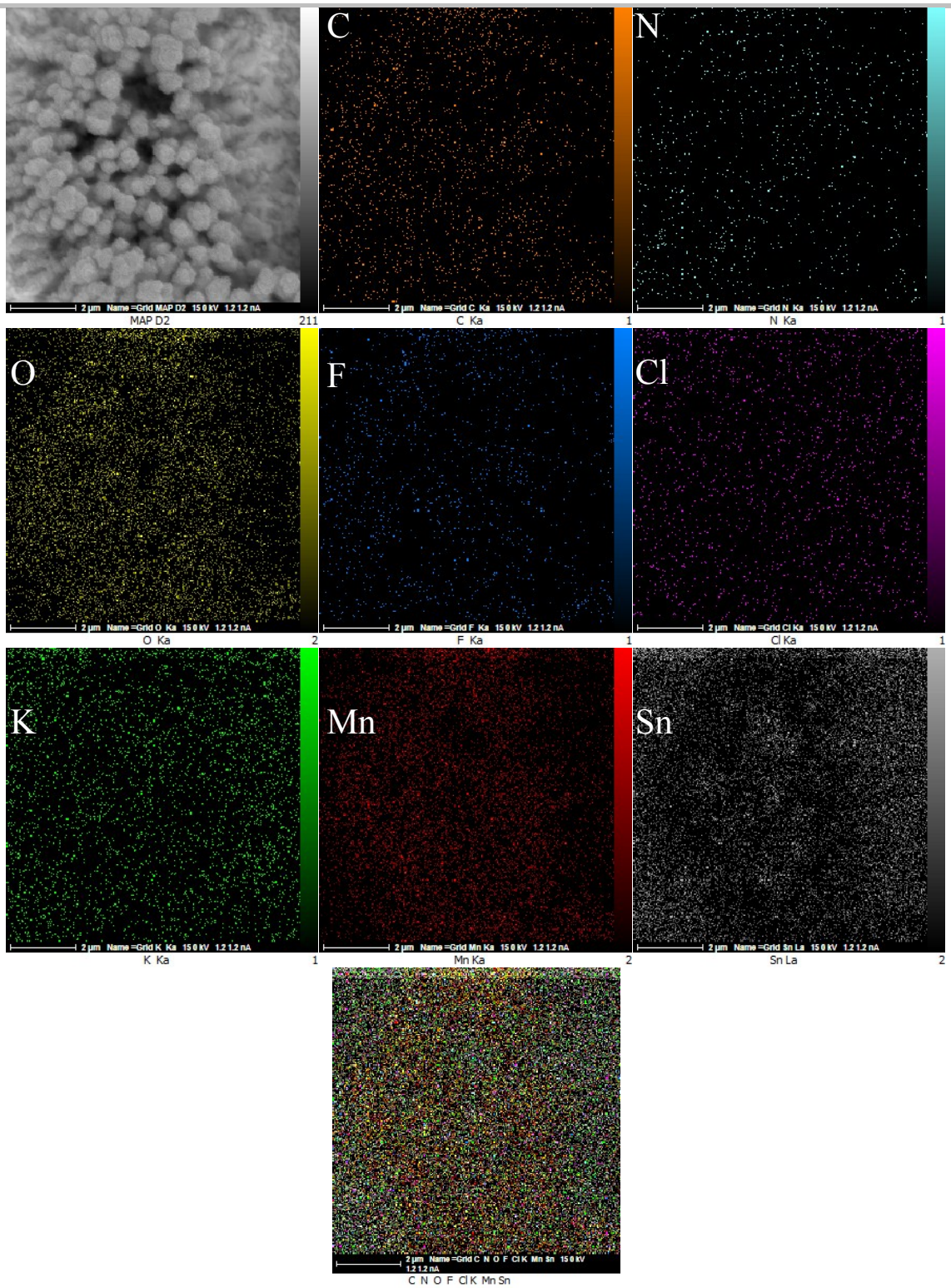

Figure S18 EDX-SEM image from FTO in the presence of phthalimide:Mn(II) with the ratio 4:1 respectively and after 2h amperometry in 0.25 M Et_4NClO_4 solution and at 1.6V. Scale bar for all images is 2 μm.

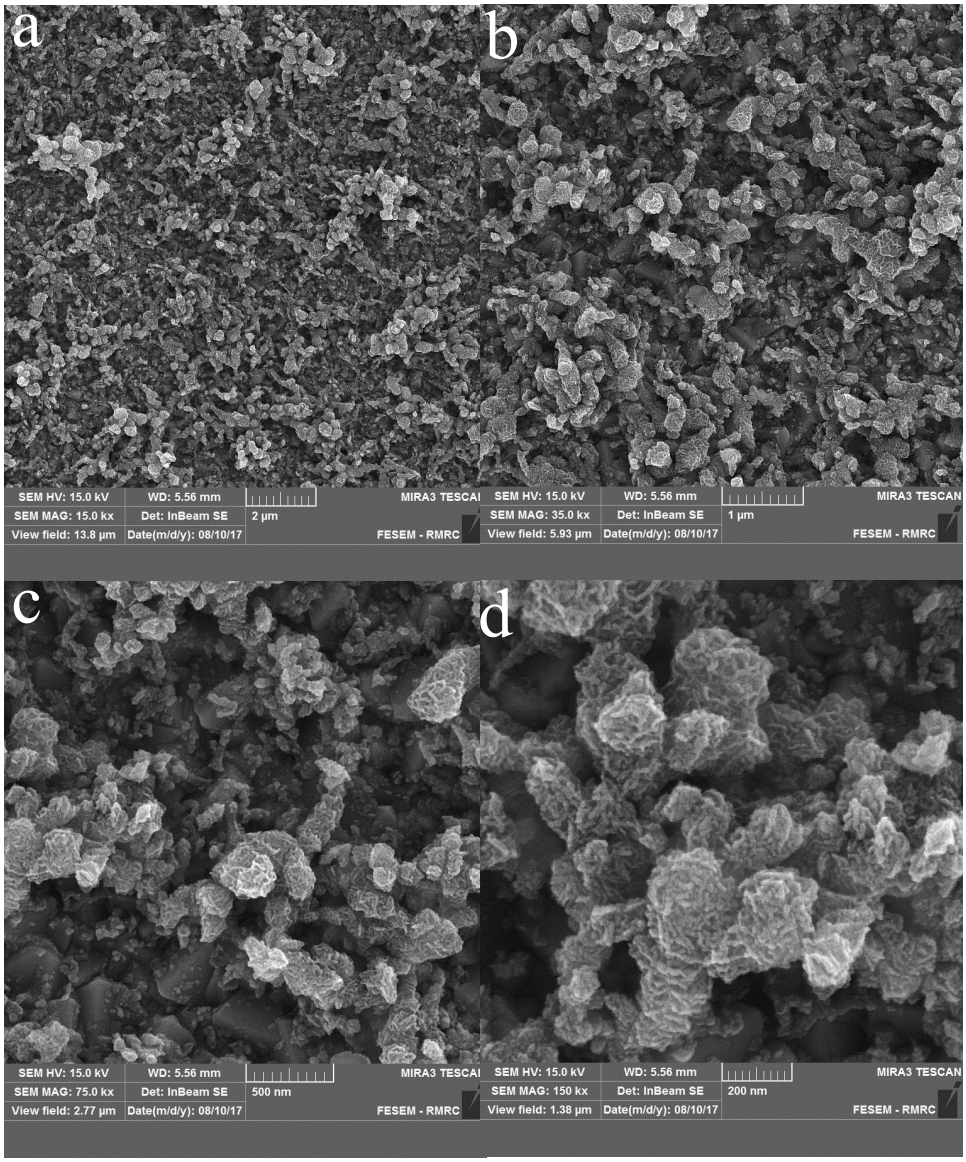

Figure S19 SEM image from FTO in the presence of phthalimide:2-cyanobenzoeic acid :Mn(II) with the ratio 2:2:1 respectively and after 2h amperometry in 0.25 M Et_4NClO_4 solution and at 1.6V (a, scale bar: 2 µm; b, scale bar: 1 µm; c, scale bar: 500 nm; d, scale bar: 200 nm).

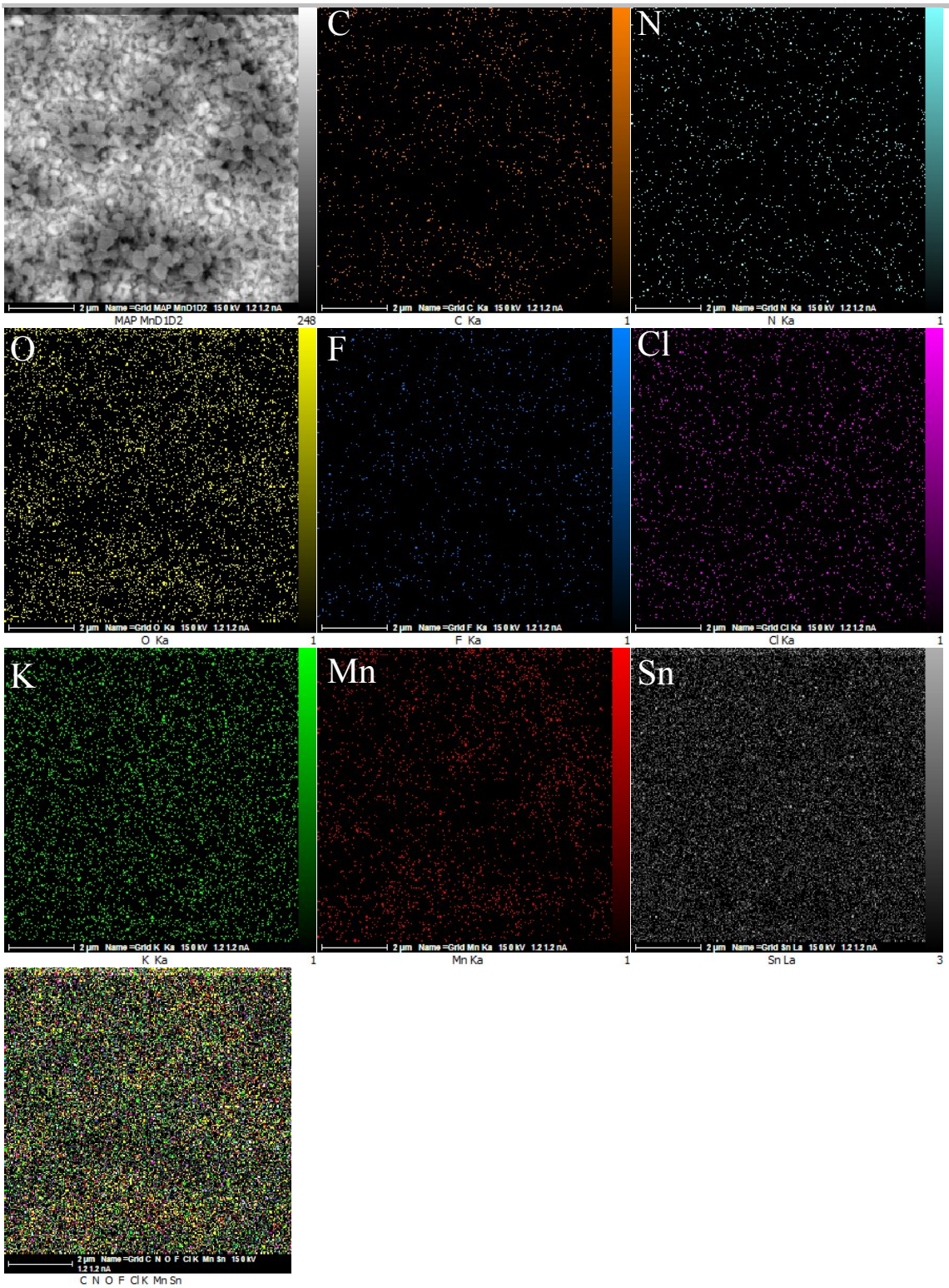

Figure S20 EDX-SEM image from FTO in the presence of phthalimide:2-cyanobenzoeic acid :Mn(II) with the ratio 2:2:1 respectively and after 2h amperometry in 0.25 M Et_4NClO_4 solution and at 1.6V. Scale bar for all images is 2 μm.

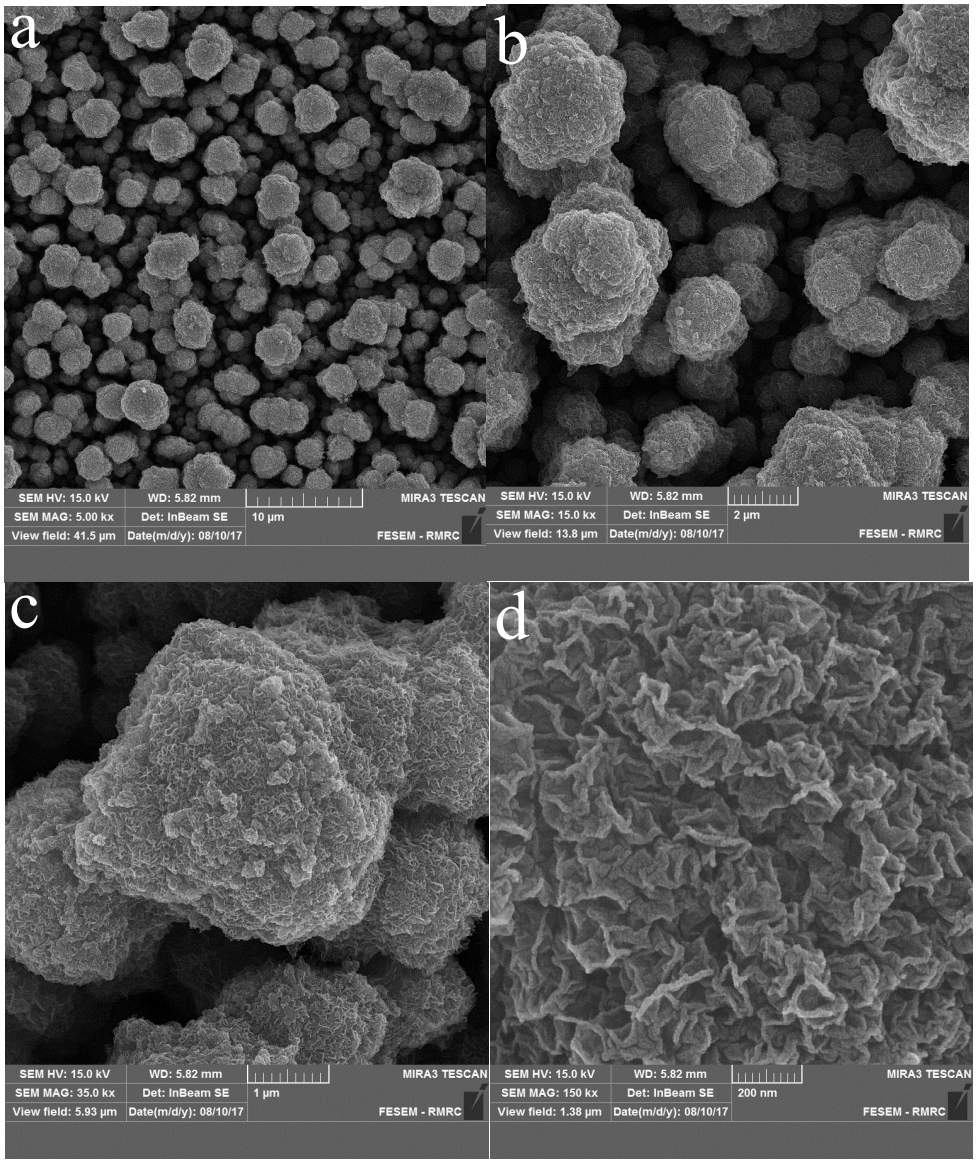

Figure S21 SEM image from FTO in the presence of phthalimide:2-cyanobenzoeic acid:Mn(II) with the ratio 2:2:1 respectively and after 10h amperometry in 0.25 M Et_4NClO_4 solution and at 1.6V (a, scale bar: 10 µm; b, scale bar: 2 µm; c, scale bar: 1 µm; d, scale bar: 200 nm)..

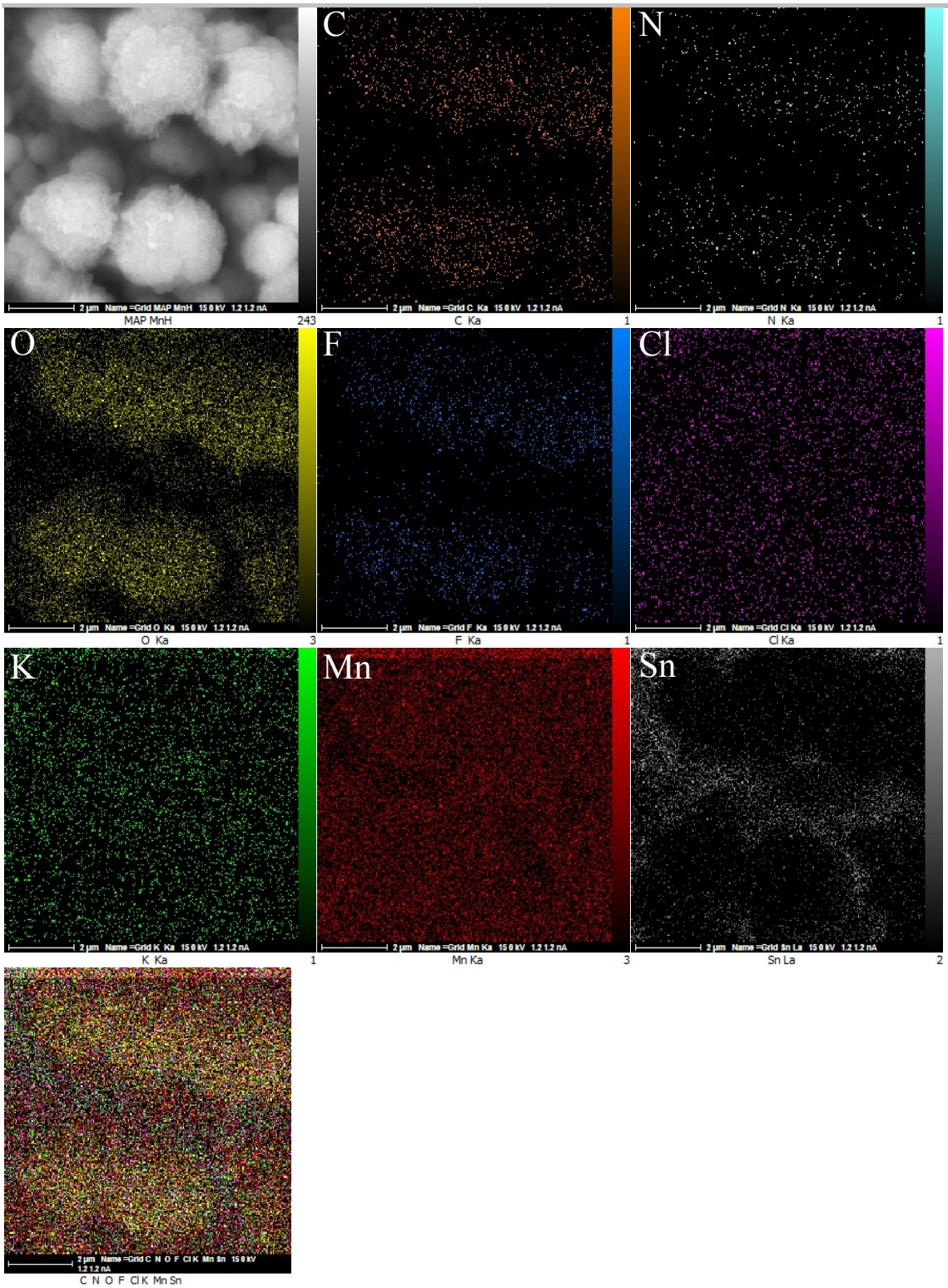

Figure S22 EDX-SEM image from FTO in the presence of phthalimide:2-cyanobenzoeic acid:Mn(II) with the ratio 2:2:1 respectively and after 10h amperometry in 0.25 M Et_4NClO_4 solution and at 1.6V. Scale bar for all images is 2 μm.

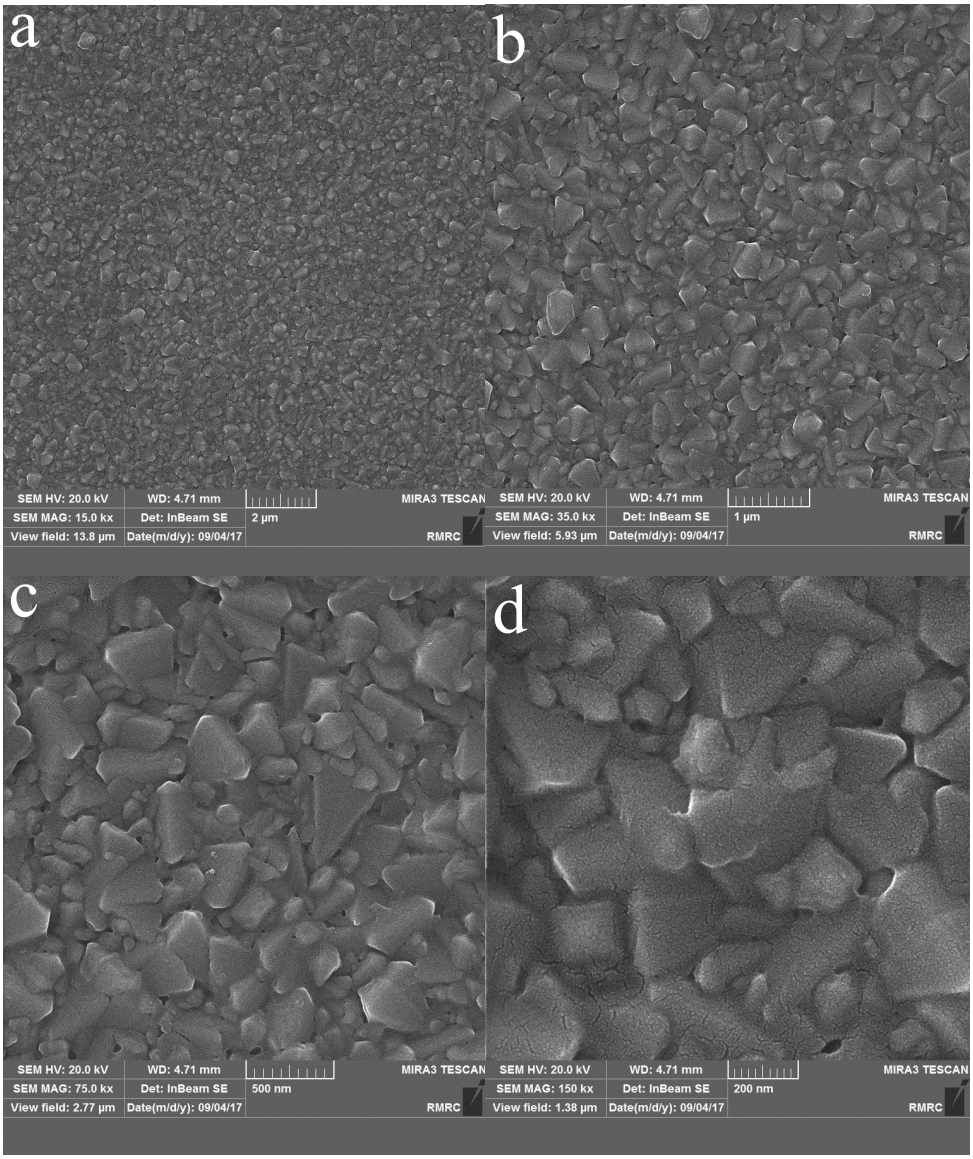

Figure S23 SEM images of FTO in the presence of **1** (0.2 mM) after 5 minutes amperometry of Et_4NClO_4 electrolyte solution (0.25 M) at 1.6V (a, scale bar: 2 µm; b, scale bar: 1 µm; c, scale bar: 500 nm; d, scale bar: 200 nm).

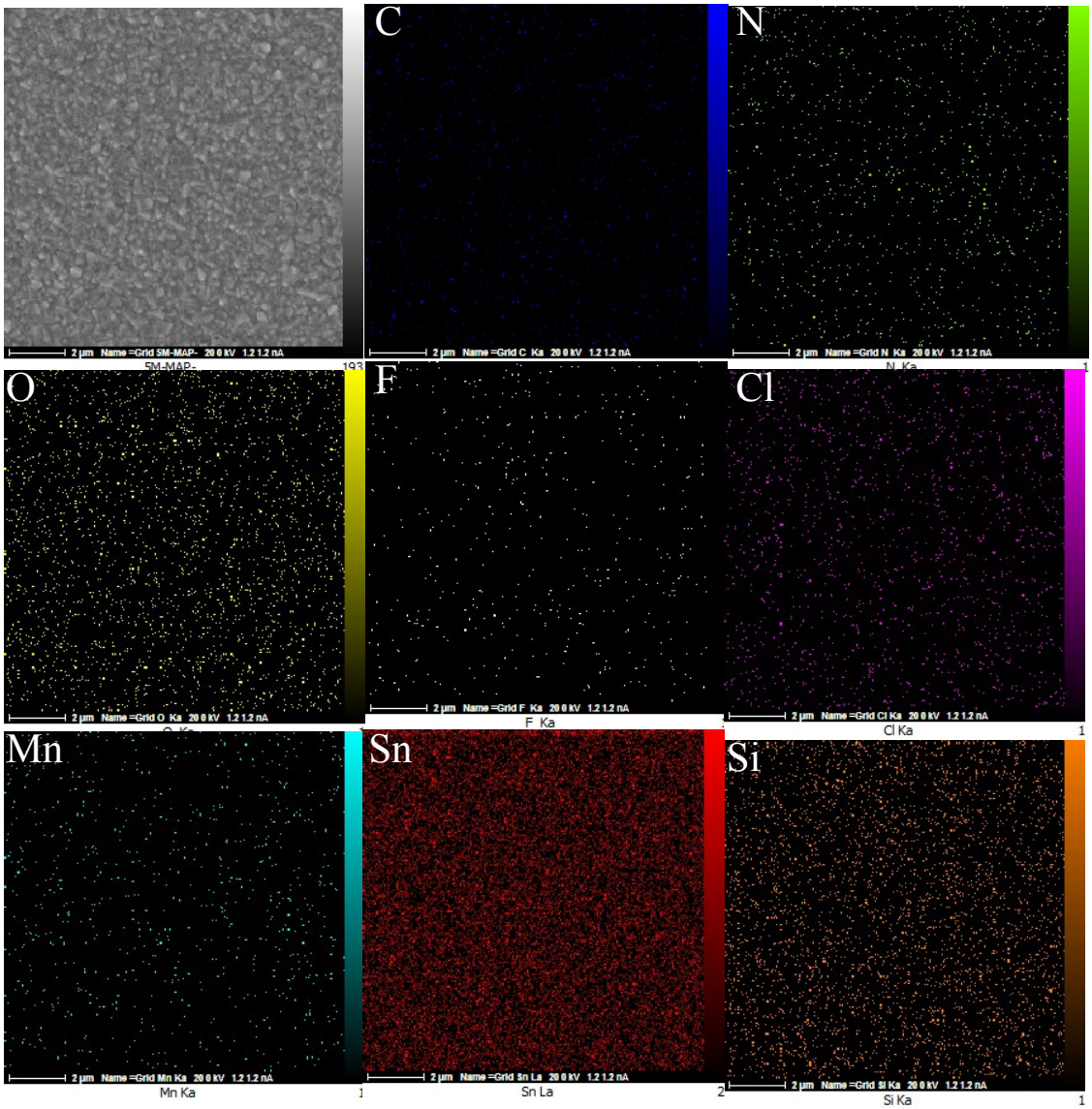

Figure S24 EDX- SEM images of FTO in the presence of **1** (0.2 mM) after 5 minutes amperometry of Et_4NClO_4 electrolyte solution (0.25 M) at 1.6V. Scale bar for all images is 2 μm.

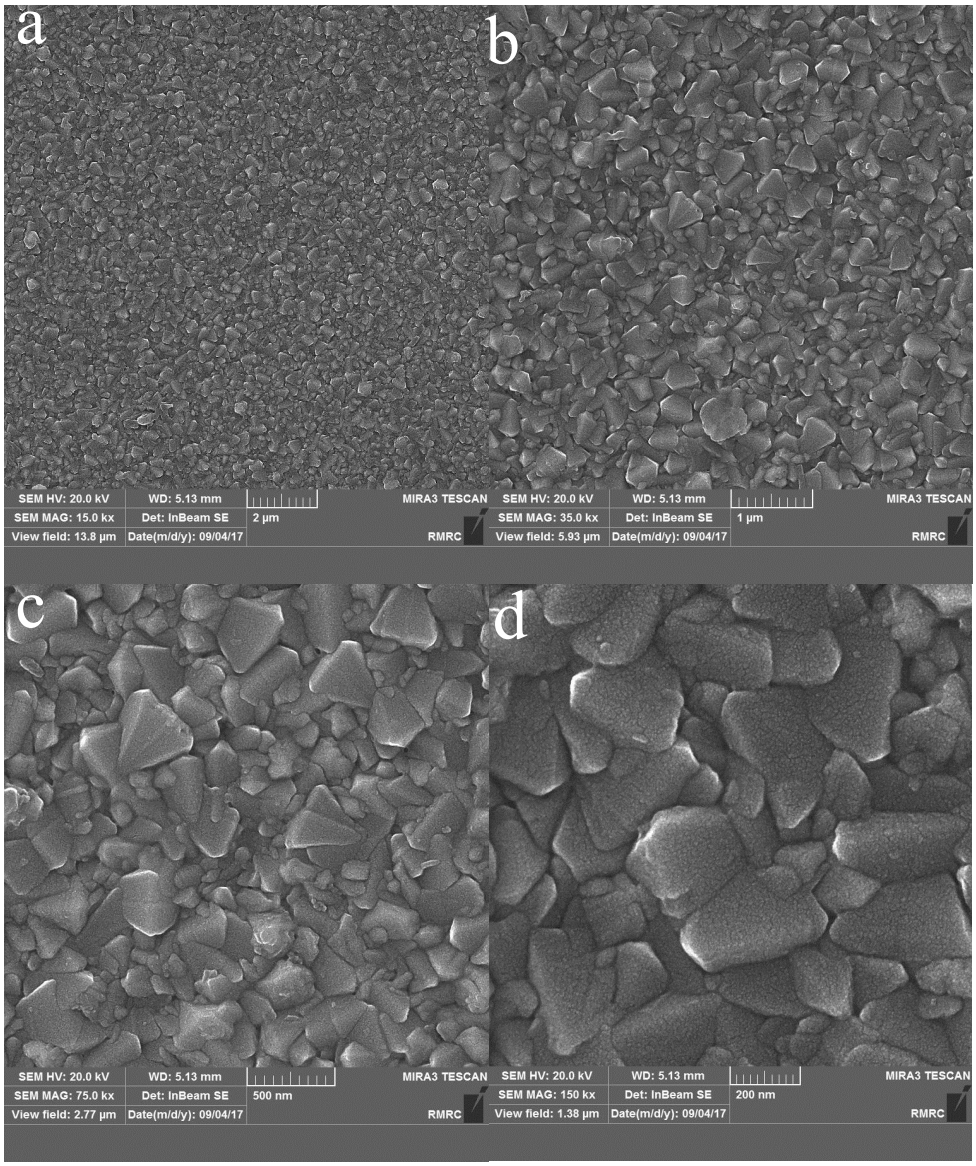

Figure S25 SEM images of FTO in the presence of **1** (0.2 mM) after 15 minutes amperometry of Et_4NClO_4 electrolyte solution (0.25 M) at 1.6V (a, scale bar: 2 µm; b, scale bar: 1 µm; c, scale bar: 500 nm; d, scale bar: 200 nm).

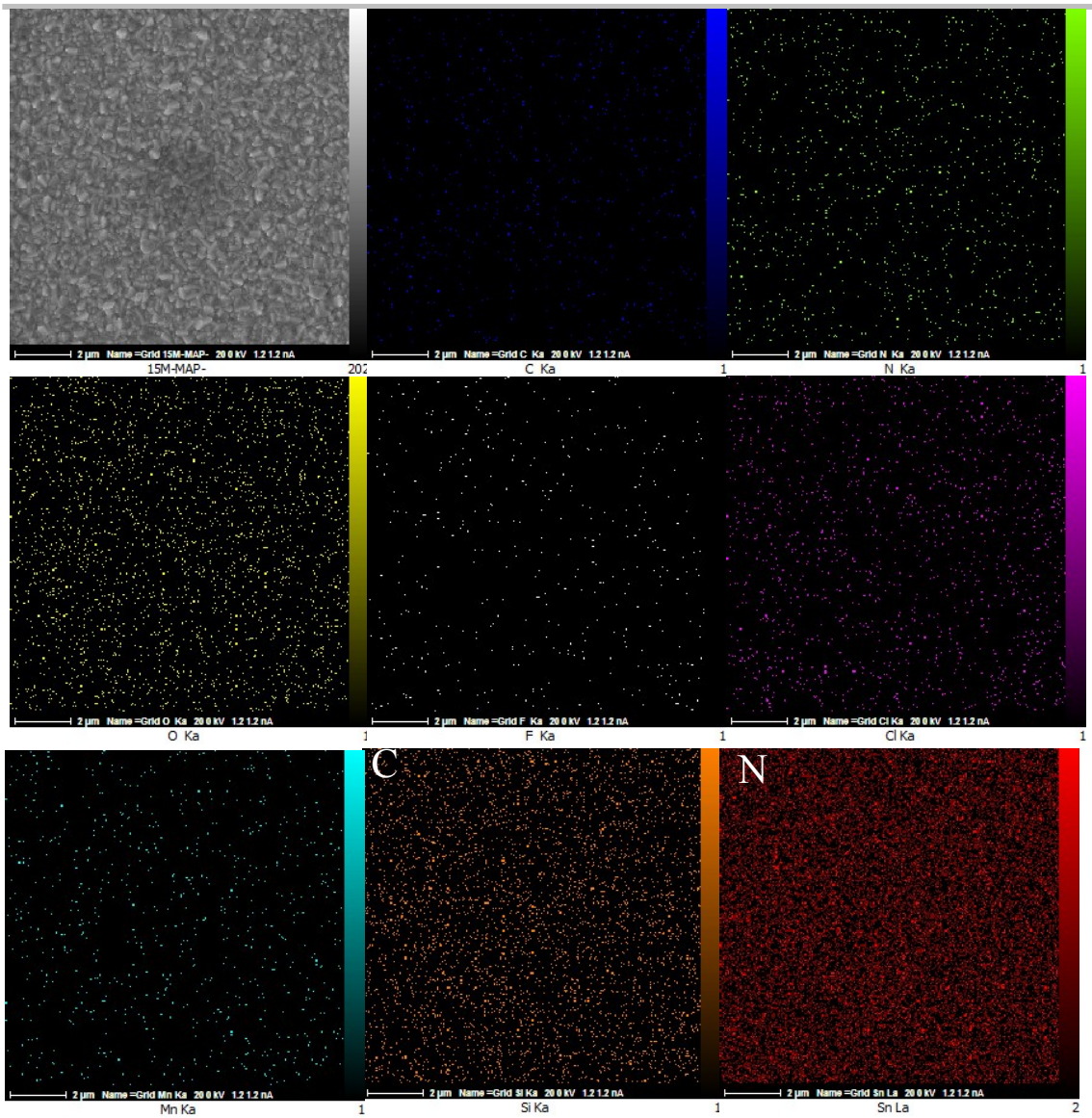

Figure S26 EDX-SEM images of FTO in the presence of **1**(0.2 mM) after 15 minutes amperometry of Et_4NClO_4 electrolyte solution (0.25 M) at 1.6V. Scale bar for all images is 2 μm.

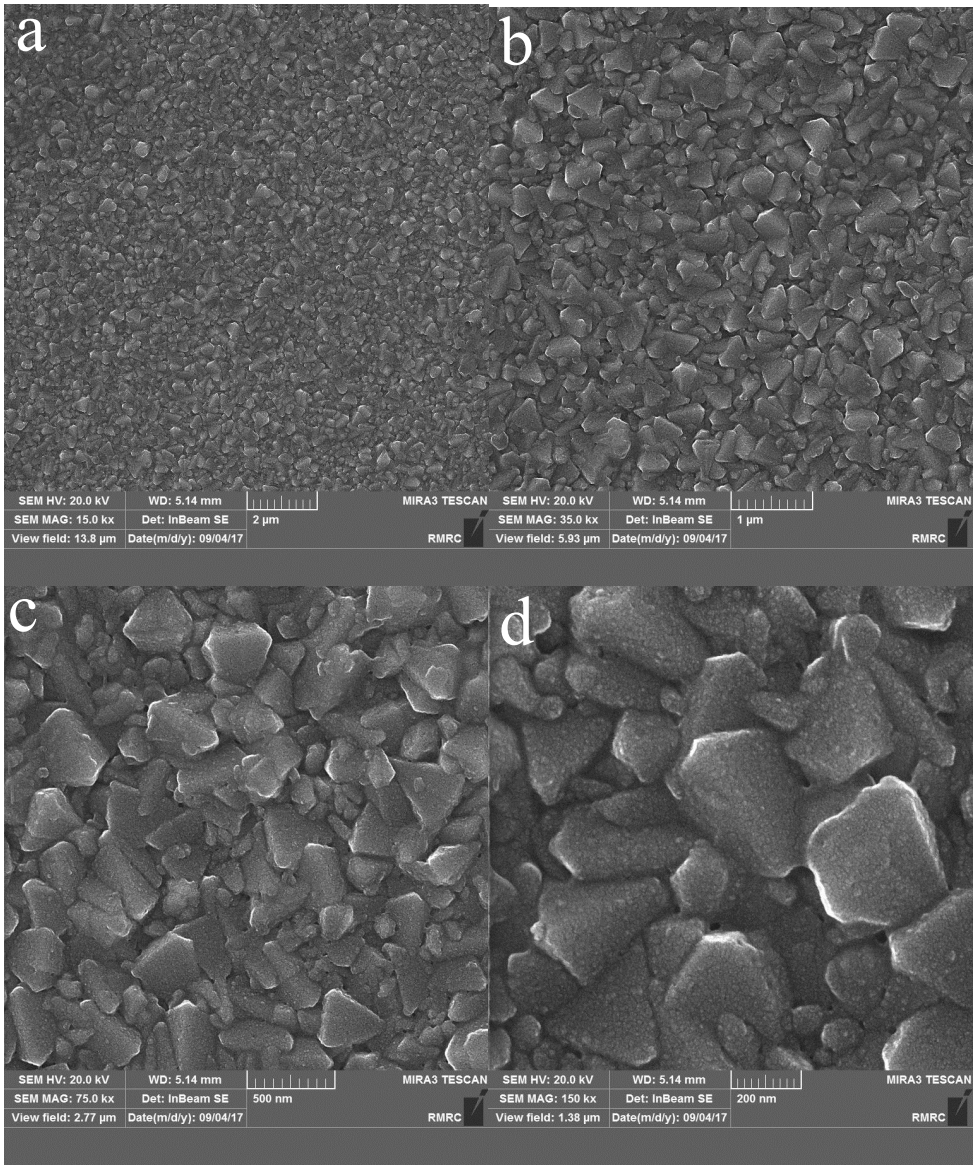

Figure S27 SEM images of FTO in the presence of **1** (0.2 mM) after 30 minutes amperometry of Et_4NClO_4 electrolyte solution (0.25 M) at 1.6V (a, scale bar: 2 µm; b, scale bar: 1 µm; c, scale bar: 500 nm; d, scale bar: 200 nm).

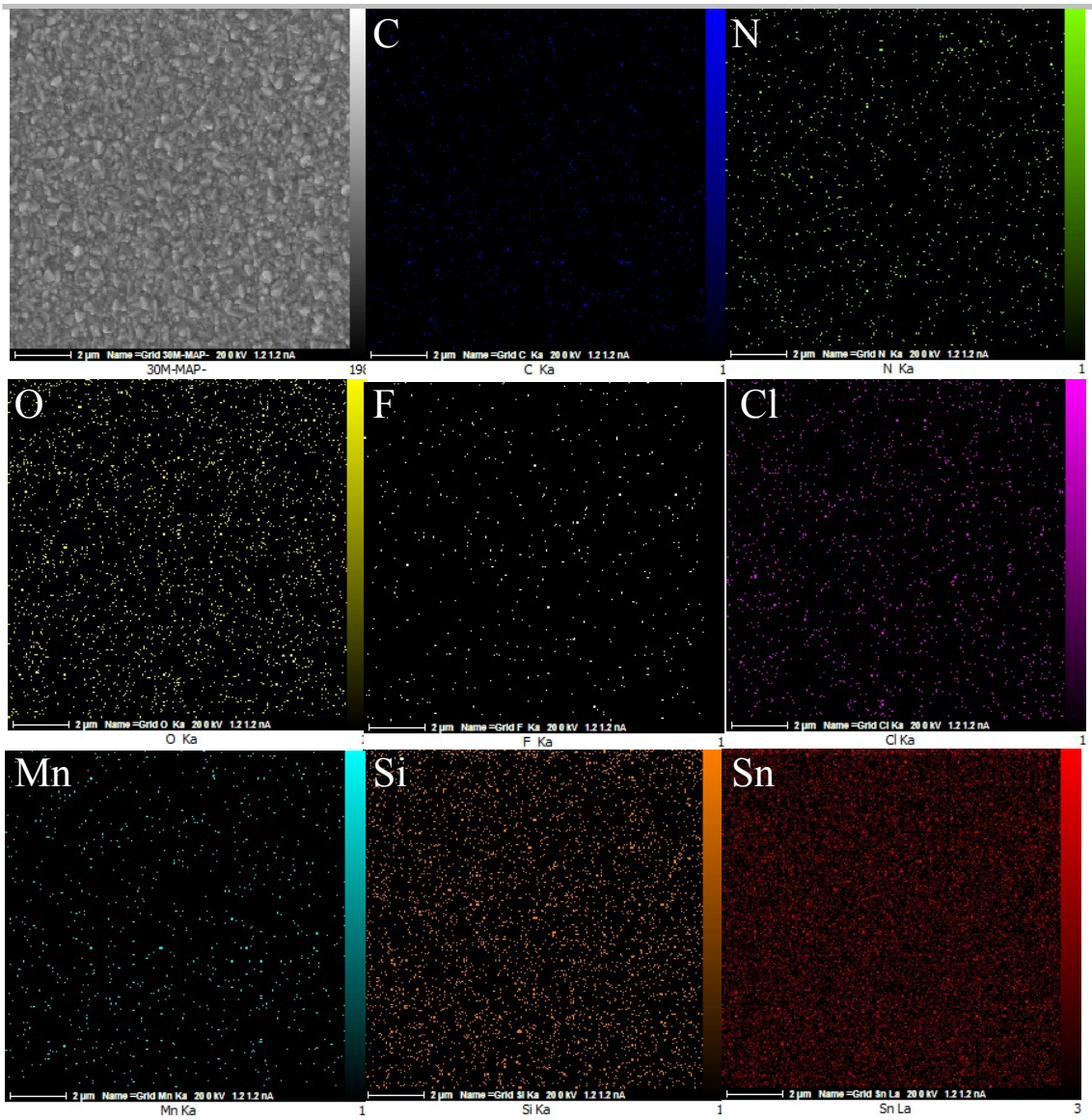

Figure S28 EDX-SEM images of FTO in the presence of **1** (0.2 mM) after 30 minutes amperometry of Et_4NClO_4 electrolyte solution (0.25 M) at 1.6V. Scale bar for all images is 2 μm.

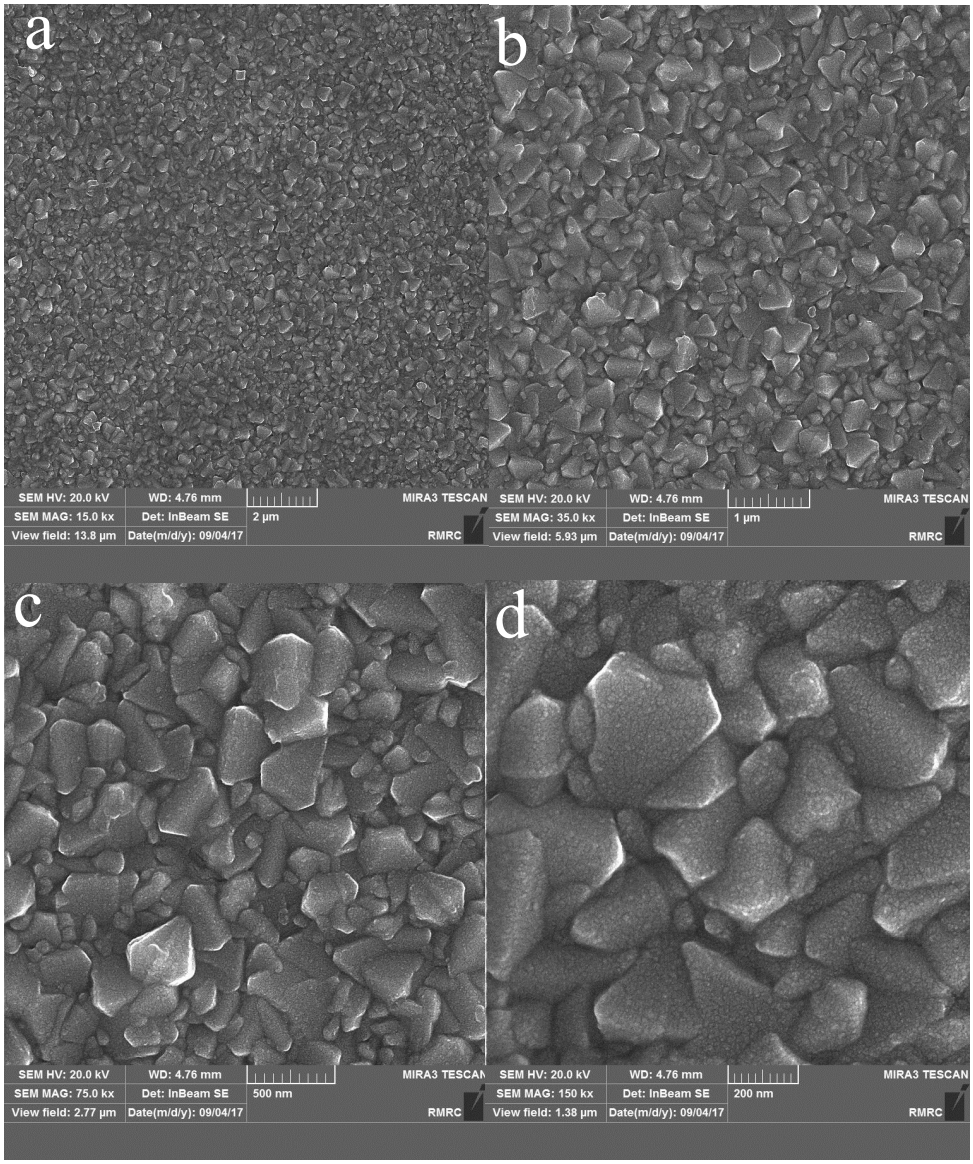

Figure S29 SEM images of FTO in the presence of **1** (0.2 mM) after one-hour amperometry of Et_4NClO_4 electrolyte solution (0.25 M) at 1.6V (a, scale bar: 2 µm; b, scale bar: 1 µm; c, scale bar: 500 nm; d, scale bar: 200 nm)..

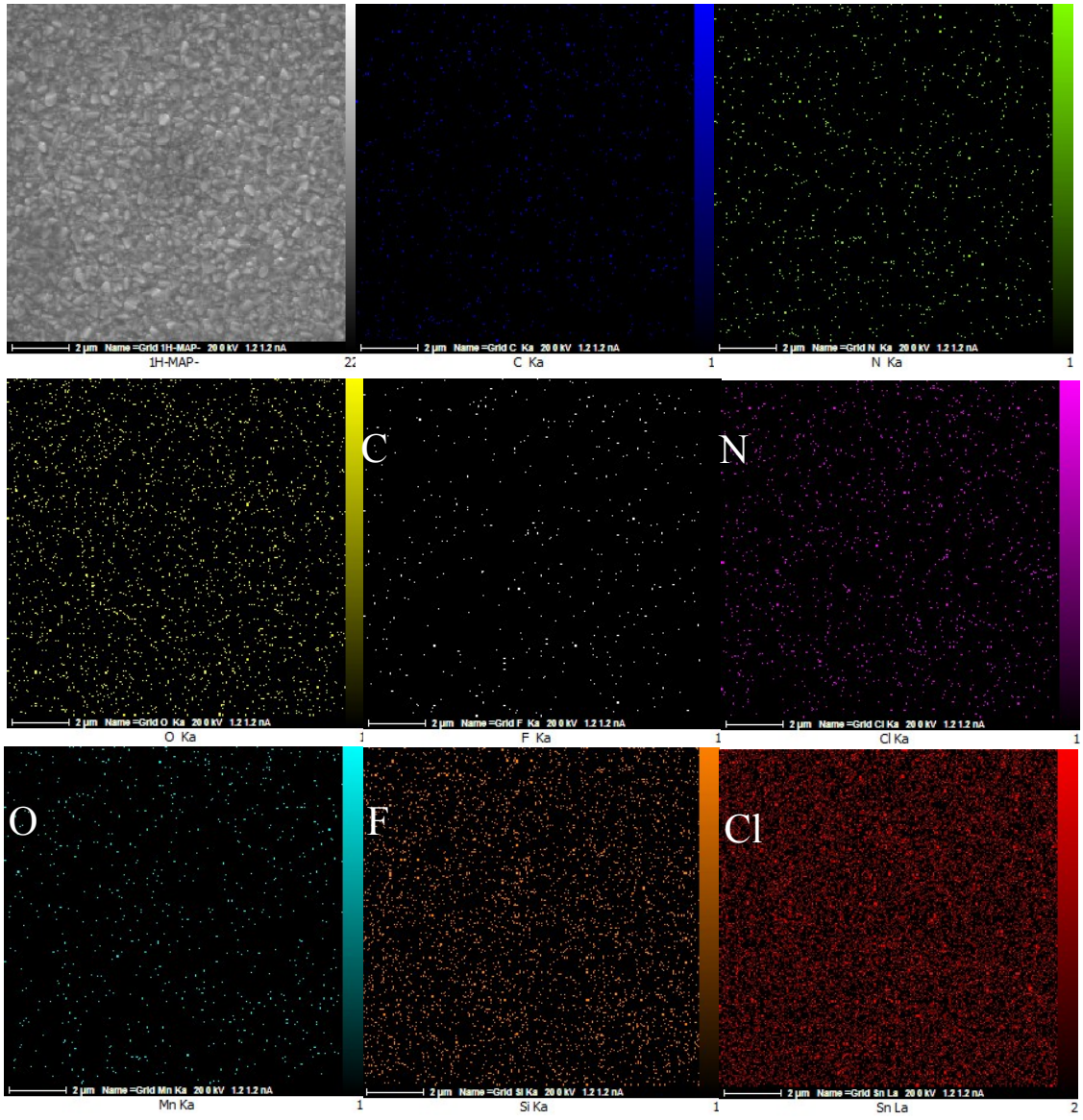

Figure S30 EDX-SEM images of FTO in the presence of **1** (0.2 mM) after one-hour amperometry of Et_4NClO_4 electrolyte solution (0.25 M) at 1.6V. Scale bar for all images is 2 μm.

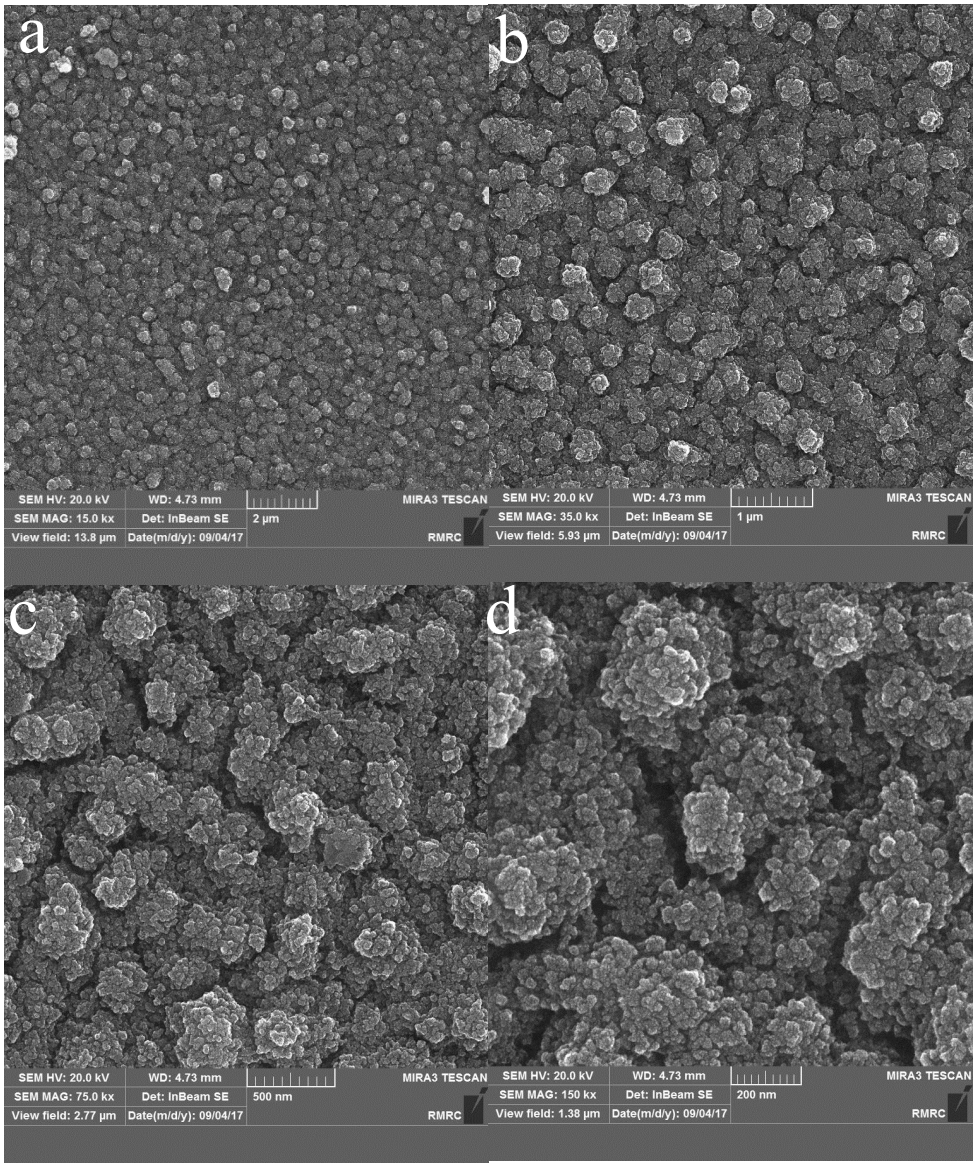

Figure S31 SEM images of FTO in the presence of **1** (0.2 mM) after 5 hours amperometry of Et_4NClO_4 electrolyte solution (0.25 M) at 1.6V (a, scale bar: 2 µm; b, scale bar: 1 µm; c, scale bar: 500 nm; d, scale bar: 200 nm).

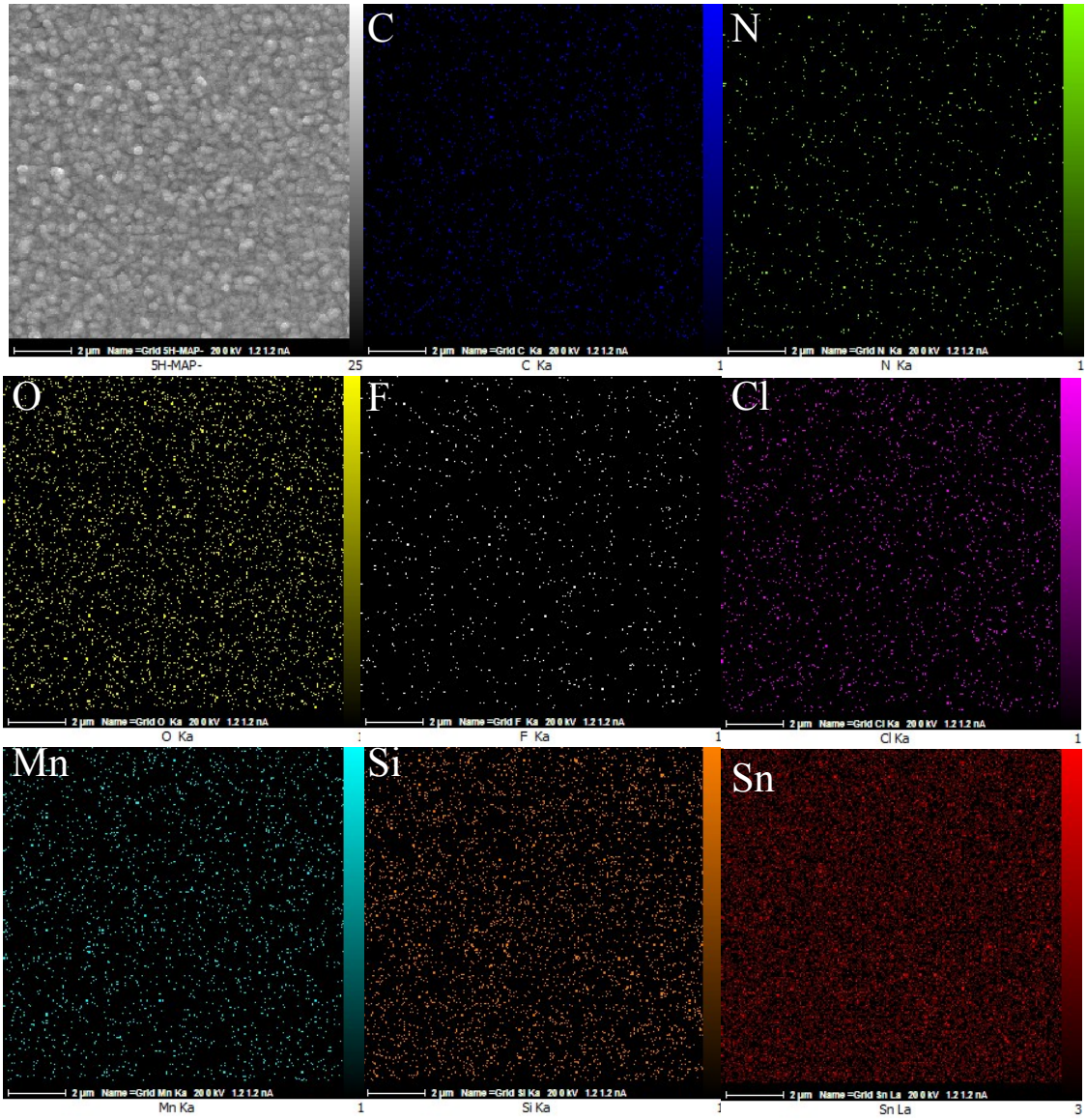

Figure S32 EDX-SEM images of FTO in the presence of **1** (0.2 mM) after 5 hours amperometry of Et_4NClO_4 electrolyte solution (0.25 M) at 1.6V. Scale bar for all images is 2 μm.

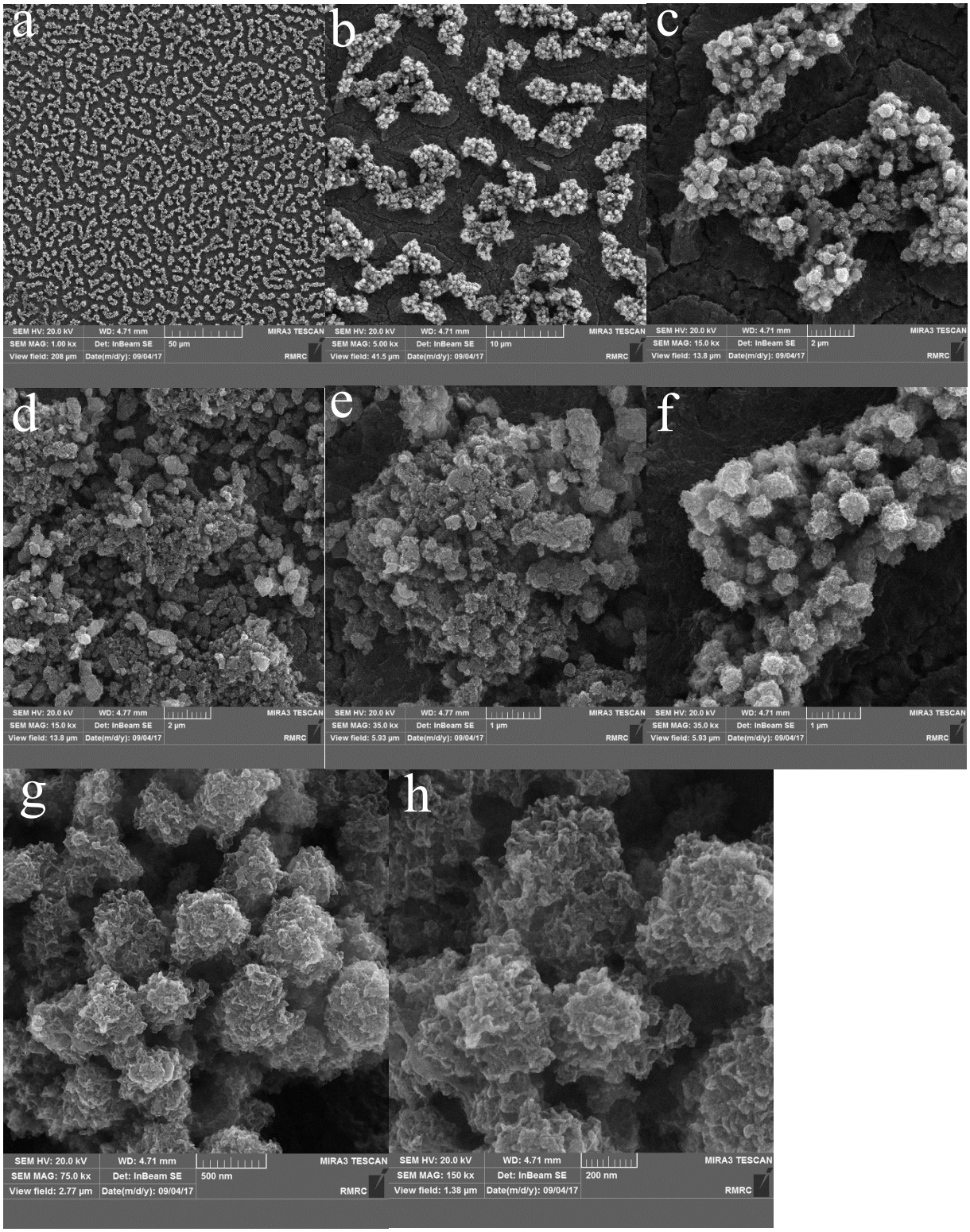

Figure S33 SEM images of FTO in the presence of **1** (0.2 mM) after 10 hours amperometry of Et_4NClO_4 electrolyte solution (0.25 M) at 1.6V (a, scale bar: 50 µm; b, scale bar: 10 µm; c, scale bar: 2 µm; d, scale bar: 2 µm; e, scale bar: 1 µm; f, scale bar: 1 µm; g, scale bare: 500 nm; h, scale bare: 200 nm).

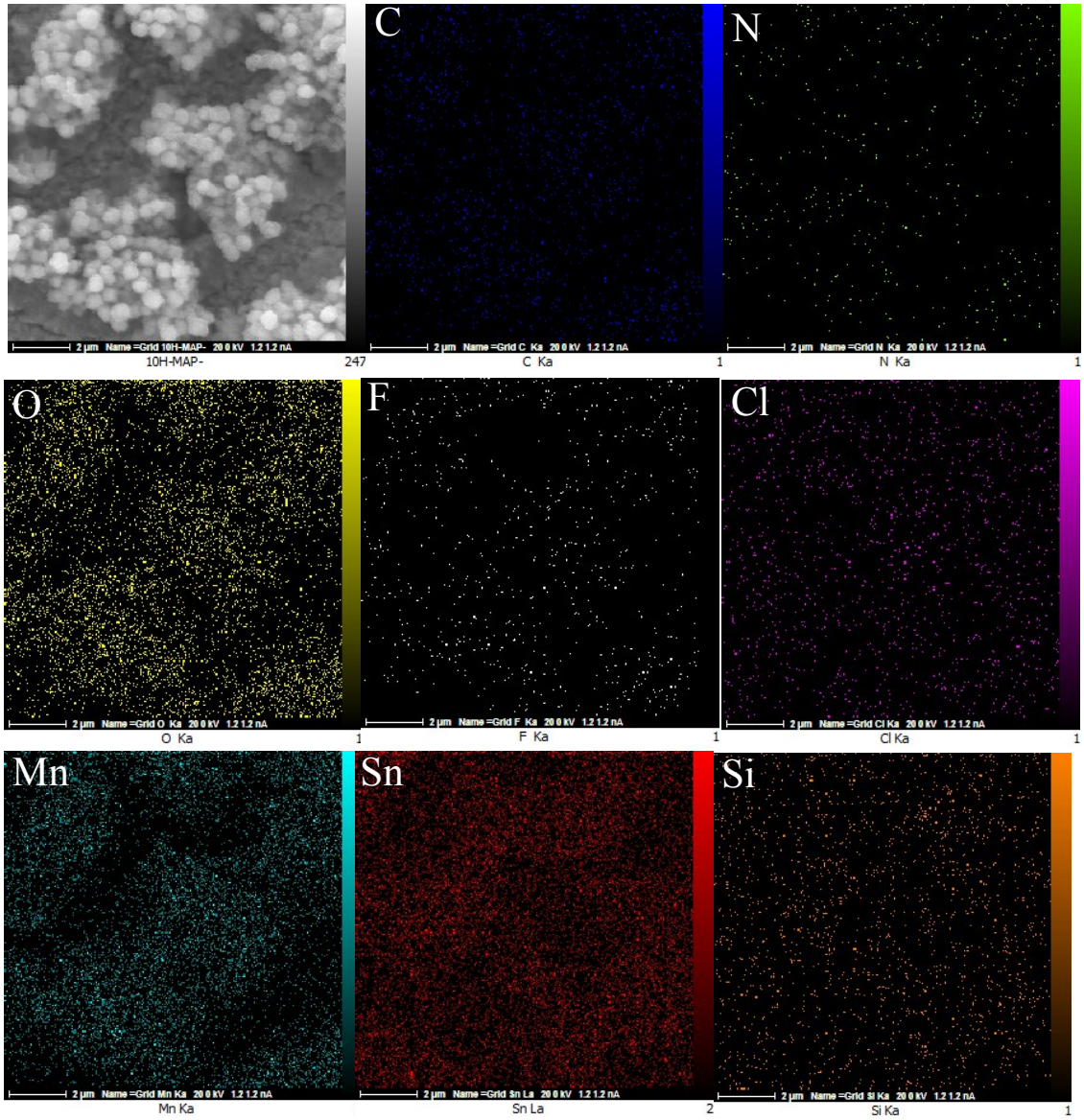

Figure S34 EDX-SEM images of FTO in the presence of **1** (0.2 mM) after 10 hours amperometry of Et_4NClO_4 electrolyte solution (0.25 M) at 1.6V. Scale bar for all images is 2 μm.

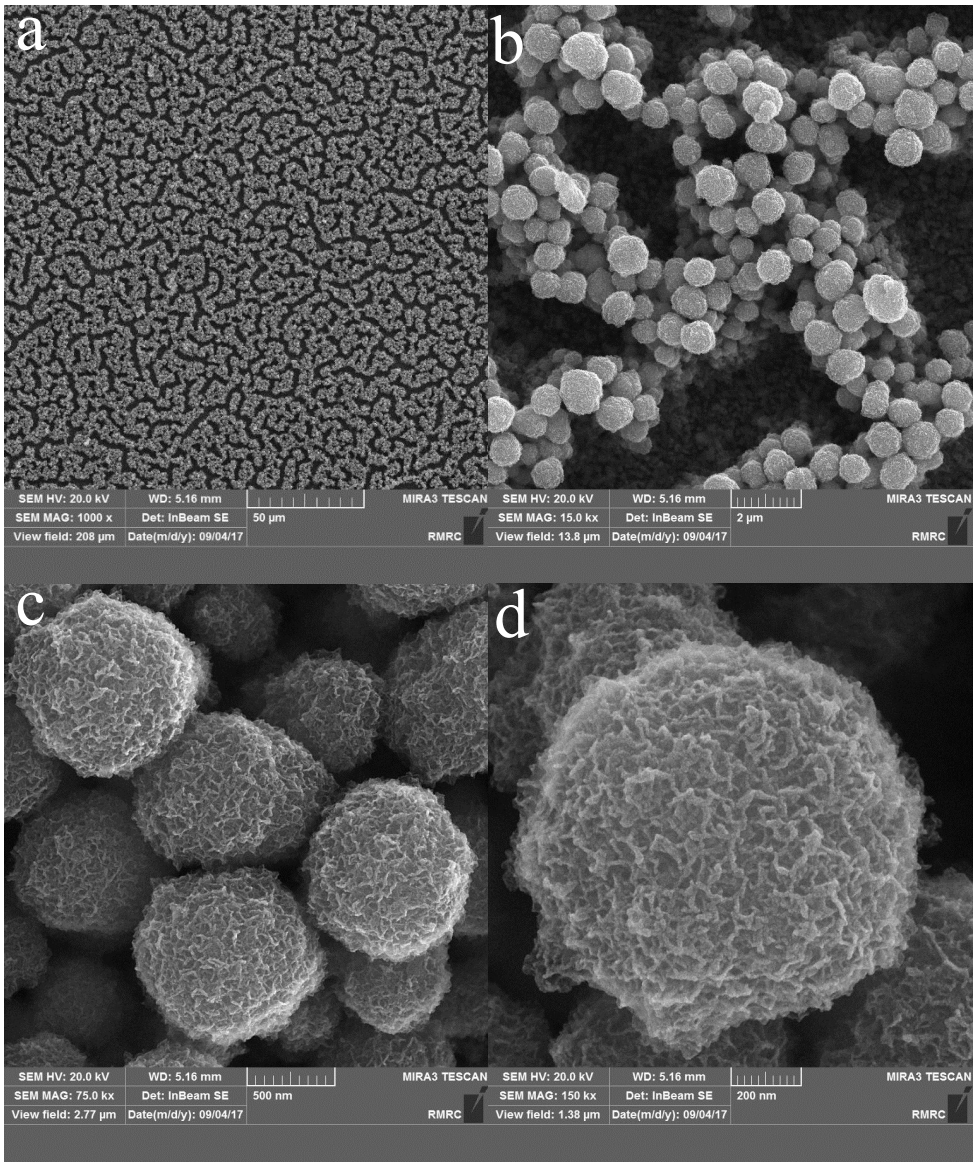

Figure S35 SEM images of FTO in the presence of **1** (0.2 mM) after 20 hours amperometry of Et_4NClO_4 electrolyte solution (0.25 M) at 1.6V (a, scale bar: 50 µm; b, scale bar: 2 µm; c, scale bar: 500 nm; d, scale bar: 200 nm).

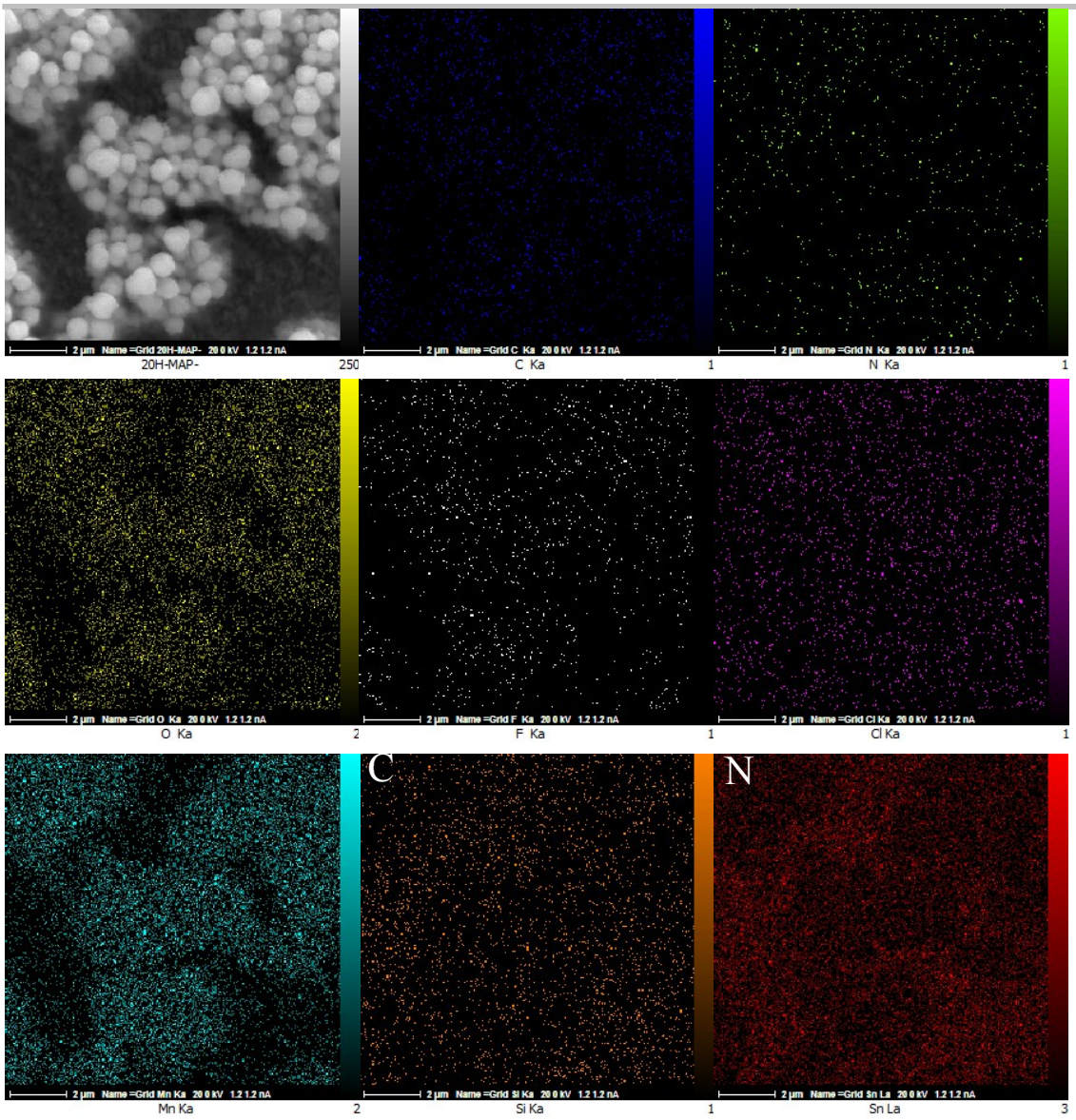

Figure S36 EDX-SEM images of FTO in the presence of **1** (0.2 mM) after 20 hours amperometry of Et_4NClO_4 electrolyte solution (0.25 M) at 1.6V. Scale bar for all images is 2 µm.

Table S1. Rates of Water Oxidation by Various Manganese Oxide Catalysts[a]

Compound	Oxidant	TOF[b]	Surface (m^2/g)	References
1	Electrochemistry (pH = 7, 1.6 V)	0.2-0.5	-	This work
Active mixed-valent MnO_x	Ce(IV)	0.16	188	3
Porous amorphous Mn oxides	Ce(IV)	0.52	184	4
Cryptomelane type tunnel Mn oxides	Ce(IV)	0.11	140	4
Layered Mn oxides	Ce(IV)	0.28	99	4
Mn_2O_3 (bixbyite)	$Ru(bpy)_3^{3+}$	0.37	16.3	5
Mn_3O_4 (hausmannite)	$Ru(bpy)_3^{3+}$	0.16	27.2	5
λ-MnO_2 (spinel)	$Ru(bpy)_3^{3+}$			5
Layered manganese-magnesium	Ce(IV)	2.2	16.8	6
Layered manganese-potasium	Ce(IV)	1.3	32.4	6
Layered manganese-cadmium	Ce(IV)	0.8	48.9	6
Nano scale manganese oxide within NaY zeolite	Ce(IV)	2.62	123.9	7
Layered manganese-aluminium or zinc oxide	Ce(IV)	1.1	Zn 92.0 Al 39.8	8
$CaMn_2O_4.H_2O$	Ce(IV)	0.54	205	9
	$Ru(bpy)_3^{3+}$	0.06	184	
Amorphous manganese oxides	Ce(IV)	0.52		3
$CaMn_2O_4.4H_2O$	Ce(IV)	0.32	303	9
MnO_2 (colloid)	Ce(IV)	0.09	-	10
α-MnO_2 nanowires	$Ru(bpy)_3^{3+}$	0.059	47	11
$CaMn_3O_6$	Ce(IV)	0.046	2.5	12
$CaMn_4O_8$	Ce(IV)	0.035	2.7	13
α-MnO_2 nanotubes	$Ru(bpy)_3^{3+}$	0.035	30	11
Mn_2O_3	Ce(IV)	0.027	7	11
β-MnO_2 nanowires	$Ru(bpy)_3^{3+}$	0.02	14.9	11
$Ca_2Mn_3O_8$	Ce(IV)	0.016	3.5	13
$CaMnO_3$	Ce(IV)	0.012	2.5	12
Nano-sized λ-MnO_2	$Ru(bpy)_3^{3+}$	0.03	42	5
Bulk α-MnO_2	$Ru(bpy)_3^{3+}$	0.01	20	5

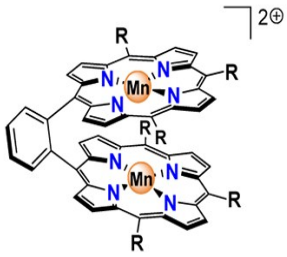	Electrochemistry	0.5	-	14
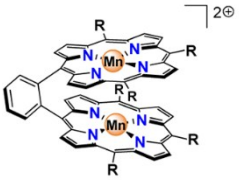 R = 4-^{t}BuC$_6$H$_4$	Electrochemistry	0.7	-	14
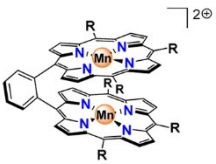 R = C_6F_5	Electrochemistry	1.8	-	14
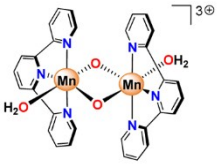	Oxone	3.3	-	15
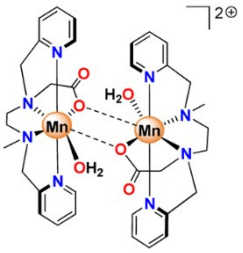	Oxone	0.6	-	16
	Oxone	0.3	-	17

	$Ru(bpy)_3^{3+}$	27	-		19
PSII	Sunlight	$1\text{-}4 \times 10^5$	-		20
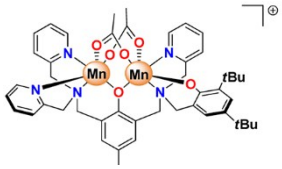	H_2O_2	5.3	-		17
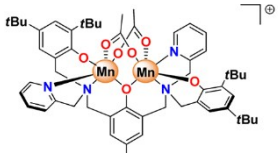	H_2O_2	3.3	-		17
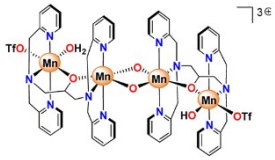	Oxone	1.8	-		17
	Oxone	3.4	-		18
	Oxone	10	-		18

[a]see also ref. 1 and 2.
[b](mmol O_2/mol Mn.s) ×10^3.

References
(1) Najafpour, M.M.; Renger, G.; Hołyńska, M.; Moghaddam, A.N., Aro; E.M., Carpentier, R. Najafpour, M.M., Renger, G., Hołyńska, M., Moghaddam, A.N., Aro, E.M., Carpentier, R.; Nishihara, H.; Eaton-Rye, J.J.; Shen, J.R.; Allakhverdiev, S.I. Chem. Rev. **2016**, 116, 2886.
(2) Kaŕkaš , M. D.; Verho, O.; Johnston, E. V.; Åkermark, B. *Chem. Rev*. **2014**, 114, 11863.
(3) Indra, A.; Menezes, P. W.; Zaharieva, I.; Baktash, E.; Pfrommer, J.; Schwarze, M.; Dau, H.; Driess, M. *Angew. Chem. Int. Ed*. **2013**, *52*, 13206.
(4) Iyer, A.; Del-Pilar, J.; King'ondu, C. K.; Kissel, E.; Garces, H. F.; Huang, H.; El-Sawy, A. M.; Dutta, P. K.; Suib, S. L. *Phys. Chem. C.* **2012**, *116*, 6474.

(5) Robinson, D. M.; Go, Y. B.; Mui, M.; Gardner, G.; Zhang, Z.; Mastrogiovanni, D.; Garfunkel, E.; Li, J.; Greenblatt, M.; Dismukes, G. C. *J. Am. Chem. Soc*.**2013**, *135*, 3494.
(6) Najafpour, M. M.; Sedigh, D. J.; Pashaei, B.; Nayeri, S. *New. J. Chem*. **2013**, *37*, 2448.
(7) Najafpour, M. M.; Pashaei, B. Dalton Trans. **2012**, 41,10156.
(8) Najafpour, M. M.; Pashaei, B.; Nayeri, S. *Dalton Trans*. **2012**, *41*, 7134.
(9) Najafpour, M. M.; Ehrenberg, T.; Wiechen, M.; Kurz, P. *Angew. Chem. Int. Ed*.**2010**, *49*, 2233.
(10) Najafpour, M. M. *Dalton Trans*. **2011**, *40*, 3805.
(11) Boppana, V. B. R.; Jiao, F. *Chem. Commun*. **2011**, *47*, 8973.
(12) Najafpour, M. M. *Dalton Trans*. **2011**, *40*, 3793.
(13) Najafpour, M. M.; Pashaei, B.; Nayeri, S. *Dalton Trans*. **2012**, *41*, 4799.
(14) Naruta, Y.; Sasayama, M. a.; Sasaki, T. *Angew. Chem. Int. Ed*. **1994**, *33*, 1839.
(15) Limburg, J.; Vrettos, J. S.; Liable-Sands, L. M.; Rheingold, A. L.; Crabtree, R. H.; Brudvig, G. W. *Science* **1999**, *283*, 1524.
(16) Poulsen, A. K.; Rompel, A.; McKenzie, C. J. *Angew. Chem., Int. Ed*. **2005**, 44, 6916.
(17)Kurz, P.; Berggren, G.; Anderlunda, M. F.; Styring, S. *Dalton Trans.* **2007**, 4258.
(18) Young, K. J.; Takase, M. K.; Brudvig, G. W. *Inorg. Chem*. **2013**, *52*, 7615.
(19) Karlsson, E. A.; Lee, B. L.; Åkermark, T.; Johnston, E. V.; Kärkäs, M. D.; Sun, J.; Hansson, Ö.; Bäckvall, J. E.; Åkermark, B. *Angew. Chem. Int. Ed*. **2011**, *50*, 11715.
(20) Yano, J.; Yachandra, V. *Chem. Rev*. **2014**, *114*, 4175.